Simulation of thermoacoustics with discontinuous Galerkin method

Michaël Gineste

Kongens Lyngby 2006

Summary

This project concerns the simulation of thermoacoustical system. The aim is to have a numerical method capable of doing broadband analysis of such system through time-domain simulation. The numerical scheme used to the spatial discretization of the governing equations is the discontinuous Galerkin method. The acoustic theory is presented, and parts of this is used to include heat effects into the numerical scheme. The resulting method is then investigated through some experiments.

Resumé

Dette projekt omhandler simulering af termoakustiske systemer. Målet er at have en numerisk metode i stand til at foretage bredbånds analyse af sådanne systemer gennem simulering i tids-domænet. Til diskretisering af den akustiske model i rummet anvendes den diskontinuerte Galerkin metode. Teorien omhandlende lyd i forbindelse med varme-udveksling er præsenteret. Nogle fysiske betragtninger bruges til at indkorporere en flukturerende varmekilde som akustiske kilde i den numeriske metode. Den resulterende metode er da undersøgt ved nogle eksperimenter.

Contents

Chapter 1

Introduction

This thesis concerns the derivation of a numerical framework, which can be used as a tool for preliminary analysis of thermoacoustic systems. As such, the numerical method has to provide the flexibility to represent a variety of different physical scenarios, and this without the need to modify the numerical scheme significantly. Such an tool can be useful to investigate the stability of the acoustical system under consideration, and eventually in an initial phase of production.

The method is used to simulate the acoustics in the time-domain, which allows for broadband excitation and following frequency analysis. So in the end, a larger picture of the model characteristics can be obtained.

The project crosses a variety of disciplines. On one hand it concerns the acoustics within a combustor (a chamber in which combustion takes place), and on the other, the use of numerical methods to solve the equation system describing the sound field in the combustor. It was based on a wish to do a project on computational aeroacoustics (CAA), a field which has many interesting challenges.

New is the field of thermoacoustics, which is the theory regarding the interaction between sound and heat. The theory is applicable to phenomena that can take place in many different devices, such as gas boilers or aeroengines.
It considers the generation of pressure waves through fluctuating heat release, e.g when a combustion process has a fluctuating part. In this project, the surroundings for the sound field is a closed system, so that the chamber acts as a

resonator and standing waves (modes) are possible. The heat input then acts as a source in this system, and this can eventually lead to acoustic instabilities under certain circumstances, where the sound pressure levels reaches very high levels and can cause structural damage or other unwanted effects. The Rijke tube phenomenon is a good example of such an thermoacoustic instability, see e.g. [3].

The theory of acoustics can be thought separated into nonlinear and linear acoustics. In this project only linear acoustics is considered so that the sound field is considered small amplitude perturbations on top of stationary values, which results in a linearization of the equations. In reality, when instabilities occur these are damped by nonlinear effects, but these are not taken into considerations here.

The numerical scheme used for the simulation is the discontinuous Galerkin (abbreviated dG) method. This is a relatively new method for solving (partial) differential equations, and was chosen because of interest and because it has some properties that makes it well-suited for aeroacoustic problems. A much used method in CAA is a dispersion-relation preserving finite difference method (Tam & Webb), but has the drawback (in my opinion) of being a low-order method. The dG method is a high-order method based on spatial discretization onto finite elements, thus it is possible to reduce the problem of inherent "numerical noise" polluting the sound field calculation. Additionally, it has good (low) dispersion error, so that it is well-suited for wave propagation. Since the goal is to use the time-domain simulation to do frequency analysis, such properties are welcome.

The justification of such a numerical tool contrary to the analytic treatment, hinges on the complexity of the acoustics, when the medium is moving, and the properties of the medium changes with temperature, and a coupling between the acoustic wave and the fluctuating heat release is present. All this affects the sound field, and closed expression is hard to obtain. Often mean flow effects are neglected by assumption of low speed flows, but might lead to expressions inadequate when also the heat release is included. Dowling showed in [1] how different (analytic) calculation methods would give different results for resonance frequencies, since especially the form of the sound-heat fluctuation coupling is difficult to incorporate. In the numerical treatment of the model, this is not a problem.

So the idea is to make a numerical "wave tank" where the sound waves are generated by a driver mechanism and a fluctuating heat release source is included. The calculations are performed in the time-domain as mentioned, thus allowing for frequency analysis over a larger spectrum, contrary to solving the wave equation in the frequency domain as a eigenvalue problem.
A key issue, both mathematically and numerically, is how to include the heat release when this is considered a compact source.

The derived method is then used to investigate some comparison cases, based on the modelling of the system.

The first chapter concerns the acoustic theory, in which the governing equations are presented and the thermoacoustic theory described. This is follow by a chapter on the numerical scheme, where the dG method is described and how the inclusion of source term is done. This is to a large extent based on the model being a hyperbolic equation system and the numerical scheme allowing discontinuities.
At last, the results of the numerical experiments is presented and conclusions of the project.

This text has been written with neither acousticians nor numerical analysists in mind, so it has been tried to explain things in a descriptive way. The notations used are sought to be standard notations within their respective framework.
The mathematical theory of hyperbolicity, which is closely related to the acoustics, is not presented although this property is used and mentioned alot. The reason being that an adequate explanation of this property would be a bit exaggeration, relative to the use of it. So it is assumed known.

Chapter 2

Governing Equations

2.1 Introduction

Here, the acoustical framework and the resulting model is presented.
It will start out with the fundamental equations concerning compressible gas dynamics, from which are derived the governing equations for the linear acoustics framework through linearization.

The modelling of the gas dynamics will be presented in one space dimension only, since the cross-sectional dimension of the chamber is considered much smaller than the acoustical wavelength. So the wave propagation is one dimensional, known as plane waves.

The equations describing the fluid motion are the conservation laws in differential form, neglecting viscosity and heat-conduction. These three conservation laws will simply be stated without derivation, which can be found in numerous textbooks.

The linearized equations are known to support three kinds of waves, referred to as acoustic waves, entropy waves, and – in higher spatial dimensions – vorticity waves. In the one dimensional case no vorticity wave exists, and will not be mentioned.

When the combustion effects comes into the acoustics, it is based on theory from thermodynamics and this theory is to a large extent not explained. So the laws of thermodynamics and the differently connections between thermodynamical state variables are used implicitly in the derivation, but not commented on.

To describe to medium in which the acoustic perturbations travel, terms like "the gas", or "the medium" are used interchangeably. Also the combustion process is called different thing; heat release, heat input or heat source are used, but all refers to the addition of energy in the form of heat.

2.2 The Euler Equations

Initially, the governing equations are presented without any source terms, which will be included later. This is done in order to make the resulting equations more physically founded

The first is conservation of mass, given as

$$\frac{\partial \rho}{\partial t} + \frac{\partial}{\partial x}(\rho u) = 0 \tag{2.1}$$

where ρ is density and u velocity. This simply states that no mass is created within the medium.

The second equation is the Navier-Stokes equation for conservation of momentum in a compressible Newtonian fluid, neglecting viscosity and heat-conduction.

$$\frac{\partial}{\partial t}(\rho u) + \frac{\partial}{\partial x}(\rho u u + p) = 0 \tag{2.2}$$

which is an representation of Newton's second law applied to the fluid control volume in regard.

The third is the energy equation, which is an application of the first law of thermodynamics to the medium. The time rate of change of total energy is equal to the rate of change in internal energy, caused by heat input to the gas, and the work done on the system. In this inviscid fluid, the only work done is by the pressure (and eventually body forces).

$$\frac{\partial}{\partial t}(\rho E) + \frac{\partial}{\partial x}(\rho E u + p u) = 0 \tag{2.3}$$

where the total energy E, the sum of internal energy and kinetic energy of the gas, is given as

$$E = e + \tfrac{1}{2}u^2 \qquad . \tag{2.4}$$

The internal energy is a function of temperature alone, again by the ideal gas assumption, and with assumed constant thermal properties (i.e. temperature independent heat capacities), gives the expression

$$e = c_V T \qquad . \tag{2.5}$$

The conservation law for total energy (2.3) can be rewritten in terms of internal energy by use of (2.4) and the momentum equation, giving

$$\frac{\partial}{\partial t}(\rho e) + \frac{\partial}{\partial x}(\rho u e) + p\frac{\partial u}{\partial x} = \rho e_{\text{heat}} \tag{2.6}$$

The internal energy equation could be the appropriate place to include the effects of additional heat release, ρe_{heat} being this source. This would dependent on the physics being considered, and in the subject considered here, the heat release is entered differently.

The three equations – (2.1),(2.2) and (2.3) – needs a fourth relation to close the system which will be the thermodynamic equation of state. By the ideal gas assumption, this is given as

$$\begin{aligned} p &= (\gamma - 1)\rho e \\ &= \rho R T \end{aligned} \tag{2.7}$$

where $\gamma = c_P/c_V$ is the ratio of specific heats and has the additional relationships

$$R = c_P - c_V \quad , \quad c_V = \frac{R}{\gamma - 1} \quad , \quad c_P = \frac{\gamma R}{\gamma - 1} \qquad . \tag{2.8}$$

Finally, the three equations form the system of conservation laws, which is how the Euler equations usually are presented. If this system was to contain additional terms (source terms), it would be called a system of balance laws or general conservation laws instead.

$$\frac{\partial U}{\partial t} + \frac{\partial F}{\partial x} = 0 \tag{2.9}$$

with

$$U = \begin{bmatrix} \rho \\ \rho u \\ \rho E \end{bmatrix} \quad , \qquad F = F(U) = \begin{bmatrix} \rho u \\ \rho u u + p \\ u\,(\rho E + p) \end{bmatrix} \tag{2.10}$$

These nonlinear partial differential allows for a variety of different phenomena, even ones which looses uniqueness and develops shocks. Therefore a solution is often sought as a weak solution to the system.
In addition, later when heat release is introduced, it enters as a Dirac's delta function, which introduces an discontinuity in the solution.

Interlude on weak solutions. The theory regarding weak solutions is a large mathematical area and quite complicated. So this short section is by far an adequate coverage of the theory, but more some principles regarding weak solutions and introduction of some conditions used throughoutly in this project.

A solution that somehow becomes discontinuous, can not fulfill the equation (2.9). Which is why we will seek an less restrictive formulation, the weak formulation. This formulation allows for the real solution (or the classic solution) to (2.9), but also for discontinuous solution.

The reasoning towards it can be expressed in different ways, but in abstract terms it tries to solve for a limit function, a function in the vicinity of the "real" function in the respective function space. A weak formulation can be defined in different ways, but one is to use test functions. This one relates to the numerical scheme presented later.
Another is presented here, to introduce some conditions used often in dealing with both the mathematical model and the numerical scheme.
The PDE in a weak formulation is defined as

$$\oint_C F \, \mathrm{d}t - U \, \mathrm{d}x = 0 \tag{2.11}$$

with C a positively oriented, piecewise-smooth, and closed curve in (x, t). If U and F are continuous and differentiable, the Green's formula in the plane gives

$$\oint_C F \, \mathrm{d}t - U \, \mathrm{d}x = \int\int_S \left(\frac{\partial U}{\partial t} + \frac{\partial F}{\partial x} \right) \mathrm{d}x \, \mathrm{d}t = 0 \tag{2.12}$$

so it is a solution to the original equation and vice versa.

Now consider the solution being discontinuous across some line in (x, t)-space, and denoting subscript $\pm$ as the limit state in front and after this shock. Using the contour C to evaluate the integral (2.11) around the shock, this can be expressed as

$$\int_{t_1}^{t_2} [F]_-^+ \, \mathrm{d}t - [U]_-^+ \, \mathrm{d}x = \int_{t_1}^{t_2} \left([F]_-^+ - \sigma \, [U]_-^+ \right) \mathrm{d}t = 0 \tag{2.13}$$

with $\sigma = \mathrm{d}x/\,\mathrm{d}t$ being the shock speed. This should hold for arbitrary t_1, t_2, which leads to that the integrand should vanish. This is known as the Rankine-Hugoniot (abbreviated RH) conditions,

$$[F]_-^+ = \sigma \, [U]_-^+ \tag{2.14}$$

which has to hold across a shock, if it is to conserve mass, momentum and energy.

The weak solution is not necessarily unique. In order to ensure a unique solution, the weak formulation is usually supplemented by an appropriate entropy

condition. In the dG method used to find a weak solution, this is incorporated in the method.

In addition, the system is hyperbolic, i.e. were (2.9) expressed in a quasi-linear form $U_t + A(U)U_x = 0$, where $A(U)$ is the jacobian matrix. Then the latter will have real and distinct eigenvalues. These eigenvalues reflects the speed at which information travels in the system. This property of hyperbolicity is quite essential in some aspects of the numerical modelling.

These conserved quantities (mass, momentum and energy) are less "physical" or natural in regard of what we hear and can measure, so the original conservation laws are formulated in a non-conservative form in terms of the primitive variables; density ρ, velocity u and pressure p. No information is lost from the equations during this change of variables.
The mass equation remains unchanged, the momentum equation in terms of velocity is derived from (2.2) by subtracting the continuity/mass conservation equation (2.1). At last, the equation describing the pressure evolution is derived from conserved internal energy equation (2.6) and the equation of state (2.7). So the system of conservation equations (2.10) in a non-conservative form, expressed in primitive quantities, is

$$\frac{\partial \rho}{\partial t} + u\frac{\partial \rho}{\partial x} + \rho\frac{\partial u}{\partial x} = 0 \tag{2.15a}$$

$$\frac{\partial u}{\partial t} + u\frac{\partial u}{\partial x} + \frac{1}{\rho}\frac{\partial p}{\partial x} = 0 \tag{2.15b}$$

$$\frac{\partial p}{\partial t} + u\frac{\partial p}{\partial x} + \gamma p\frac{\partial u}{\partial x} = 0 \tag{2.15c}$$

This change of variables does change the elements in the coefficient matrix of the system (2.15), but not its structure, since this coefficient matrix and the jacobian matrix mentioned earlier are conjugate.

The eigenvalues of this system are

$$\lambda_1 = u - c \ , \ \lambda_2 = u \ , \ \lambda_3 = u + c \tag{2.16}$$

which reflects two sound waves travelling at their characteristic speeds λ_1 and λ_3 down- and upstream respectively, and one convective-acoustic wave λ_2 in the system.

2.3 The Linearized Euler Equations

In order to simplify things and to decouple the acoustics from the aerodynamics, the variables describing the gas dynamics are considered separated into a stationary, equilibrium field and a much smaller time-dependent, acoustic perturbation.

$$\begin{array}{llll} \text{pressure} & : p(x,t) = \bar{p}(x) + p'(x,t) & \text{, density} & : \rho(x,t) = \bar{\rho}(x) + \rho'(x,t) \\ \text{velocity} & : u(x,t) = \bar{u}(x) + u'(x,t) & \text{, temperature} & : T(x,t) = \bar{T}(x) + T'(x,t) \\ \text{entropy} & : s(x,t) = \bar{s}(x) + s'(x,t) & & \end{array}$$

which can be justified if the perturbations are small relative to the stationary values e.g. $p'/\bar{p} \ll 1$, which is the case as long as we're considering sound pressure levels below human threshold ~ 140dB. These stationary fields are the fields generally refered to when the term 'mean' is used, e.g. mean flow velocity is $\bar{u}$.

Inserting these separated quantities into the equations (2.15), neglecting higher-order terms, and subtracting the equations (2.15) for the mean values, results in the so-called linearized Euler equations (LEE) for the acoustic field. Note that this procedure implies that the mean flow satisfies the original equations.
This results in the system

$$\begin{bmatrix} \rho' \\ u' \\ p' \end{bmatrix}_t + \begin{bmatrix} \bar{u} & \bar{\rho} & 0 \\ 0 & \bar{u} & 1/\bar{\rho} \\ 0 & \gamma\bar{p} & \bar{u} \end{bmatrix} \begin{bmatrix} \rho' \\ u' \\ p' \end{bmatrix}_x + \begin{bmatrix} \bar{u}_x & \bar{\rho}_x & 0 \\ \bar{u}\bar{u}_x/\bar{\rho} & \bar{u}_x & 0 \\ 0 & \bar{p}_x & \gamma\bar{u}_x \end{bmatrix} \begin{bmatrix} \rho' \\ u' \\ p' \end{bmatrix} = \begin{bmatrix} 0 \\ 0 \\ 0 \end{bmatrix} \tag{2.17}$$

Hence the mean flow gradients, if present, will act as additional source terms in the system.

When the medium is at rest (stagnant), the linearized mass and momentum equation, along with the energy equation $\partial s'/\partial t = 0$, gives the equations that describes the acoustics in the medium

$$\begin{bmatrix} u' \\ p' \end{bmatrix}_t + \begin{bmatrix} 0 & 1/\bar{\rho} \\ \gamma\bar{p} & 0 \end{bmatrix} \begin{bmatrix} u' \\ p' \end{bmatrix}_x = \begin{bmatrix} 0 \\ 0 \end{bmatrix} \quad , \tag{2.18}$$

which is the equation system used as limit of a vanishing flow. Mean pressure is constant in absence of flow and obviously there is no convected entropy wave.

Along these linearized equations are the linearized state equations/thermodynamic

relations

$$p' = \frac{\bar{p}}{\bar{\rho}}\rho' + \frac{\bar{p}}{\bar{T}}T' \quad = \bar{c}^2\rho' + \frac{\bar{\rho}\bar{c}^2}{c_P}s' \tag{2.19}$$

$$s' = \frac{c_V}{\bar{p}}\left(p' - \bar{c}^2\rho'\right) = c_P\left(\frac{T'}{\bar{T}} - \frac{(\gamma-1)p'}{\gamma\bar{p}}\right) \tag{2.20}$$

and variations of these.

The squared sound speed is defined as $\partial p/\partial\rho|_s$, which for a perfect gas gives the usual expression

$$c^2 = \frac{\gamma p}{\rho} \tag{2.21}$$

The linearization gives, in principle, fluctuations in this sound speed, but these are ignored, and thus $c^2 = \bar{c}^2 = \gamma\bar{p}/\bar{\rho}$ is the definition of the sound speed used throughoutly.

The linearization evidently removes the nonlinearity, but also makes the flux coefficient matrix (locally) constant in contrast to earlier, while the mathematical structure/wave nature remains the same (i.e. it is still hyperbolic), so the eigenvalues are the same, although given by the mean flow values only.

Thus the equations (2.17) (or (2.18) for stagnant medium) constitutes the governing equations for the sound field in this project. This system of PDEs is considered over the domain $(x,t) \in [0,L] \times \mathbb{R}^+$ by the plane waves assumption, along with appropriate boundary conditions. The number of conditions imposed at a boundary is determined by whether the boundary is an inlet or an outlet. In the following $\bar{u}(x) > 0$, so $\hat{\boldsymbol{n}}\bar{u}(0) < 0$ and $x_{\text{IN}} = 0$ is the inlet and $x_{\text{OUT}} = L$ the outlet.
Additionally, the flow is considered subsonic throughout the domain, so the local Mach number $M(x) = \bar{u}(x)/\bar{c}(x)$ is always <1.

The system requires boundary conditions in order to be well-posed and to describe the physical surroundings. The number of required boundary conditions are prescribed by the number of entering characteristics, with respect to the boundary normal. The mean flow enters at the left boundary, so two characteristics are incoming ($\lambda_2 = \bar{u}$ and $\lambda_3 = \bar{u} + \bar{c}$), hence two boundary conditions are needed here. While at the outlet, only one characteristic is incoming $\lambda_1 = \bar{u} - \bar{c}$, so here only one boundary condition is required.

The simplest conditions are those describing open and closed ends of the duct. These are still idealised describtions but sufficient for the purpose.
Later in this report, the condition imposed at the outlet is that of being an open end (also called pressure release), which is represented by requiring the pressure

fluctuation to vanish.

$$p'(x_{\text{OUT}}, t) = 0 \tag{2.22}$$

Were this considered a closed end, this is equivalent to requiring the fluctuation velocity to vanish

$$u'(x_{\text{OUT}}, t) = 0 \tag{2.23}$$

Such conditions give rise to reflections, the open end gives an acoustic wave reflection in antiphase of the incoming, while the closed end reflects the incoming wave in phase. A third possibility (in term of reflection) is obviously no reflection, which can be expressed by stating that the boundary impedance is the characteristic impedance of the medium. Imposing boundary conditions in a numerical scheme in term of impedance conditions is a study for itself, and if non-reflecting boundaries were needed, the boundary formulation would depend on other aspects of the model i.e. its hyperbolicity.

Another condition used is that of the flow being choked. This can be expressed in the form of a zero fluctuating mass-flux

$$\bar{u}\rho' + u'\bar{\rho} = 0 \tag{2.24}$$

This kind of boundary condition implies something about the inlet geometry. A boundary conditions of this kind is used to describe that the incoming flow passes through a nozzle.

Another used condition at the inlet is that the inflow is isentropic. If no entropy fluctuation exists at the inlet, the sound field will be isentropic until it passes some source (explained later). So if we want the incoming sound field with respect to the flame to be isentropic, the boundary condition has to ensure isentropicity. The approach taken here is to use the relation $p' = \bar{c}^2\rho'$ in some way.

Nondimensional Equations

The linearized Euler equation can be put into nondimensional form, where the mean flow influence is characterized by the Mach number. The following scalings are introduced

$$\tilde{\rho} = \frac{\rho'}{\rho_0}\ ,\ \tilde{u} = \frac{u'}{c_0}\ ,\ \tilde{p} = \frac{p'}{\rho_0 c_0^2}\ ,\ \tilde{x} = \frac{x}{L}\ ,\ \tilde{t} = \frac{t}{L/c_0} \tag{2.25}$$

where the subscript '0' refers to mean flow values at the inlet. Inserting and dividing through with the diagonal matrix

$$S = \text{diag}\left(\frac{L}{\rho_0 c_0}, \frac{L}{c_0^2}, \frac{L}{\rho_0 c_0^3}\right) \tag{2.26}$$

results in the system of non-dimensional equations

$$\begin{bmatrix}\tilde{\rho}\\ \tilde{u}\\ \tilde{p}\end{bmatrix}_t + \begin{bmatrix}M & 1 & 0\\ 0 & M & 1\\ 0 & 1 & M\end{bmatrix}\begin{bmatrix}\tilde{\rho}\\ \tilde{u}\\ \tilde{p}\end{bmatrix}_x + \frac{L}{c_0}\begin{bmatrix}\bar{u}_x & c_0\bar{\rho}_x/\rho_0 & 0\\ M\bar{u}_x/\bar{\rho} & \rho_0\bar{u}_x/c_0 & 0\\ 0 & \bar{p}_x/\rho_0 c_0 & \gamma\bar{u}_x\end{bmatrix}\begin{bmatrix}\tilde{\rho}\\ \tilde{u}\\ \tilde{p}\end{bmatrix} = \begin{bmatrix}0\\ 0\\ 0\end{bmatrix} \tag{2.27}$$

where $M = \bar{u}(x)/c_0$ is the local Mach-number.
Such an nondimensionalization is useful to reduce the different scalings in the system, and can be appropriate in many cases when a physical problem is dealt with numerically, since it reduces the potential scale disparities. For the purpose here, where the acoustics are simulated in time to obtain time-series, this would be benificial if a low-order numerical scheme was used, where the low scales of acoustic perturbations might drown in numerical noise (round-off errors and such). But such an nondimensionalization also scales the frequency (by the time scaling), and most importantly the resulting wavelength. A general rule-of-thumb in numerical analysis is that the domain discretization should allow for at least 5 grid-points per wavelength in order to resolve a wave, and thus the spatial discretization becomes very fine and hence computationally more expensive. So later when then governing equations are discretized, they will be in dimensional form, although the scaling presented above are used in some aspects of the method.

When the heat release is introduced in the equations, an appropriate scaling could be taken as energy density per time.

2.4 Heat Release

The acoustical theme of this project is thermoacoustics, a term implying that we consider the conversion of energy in form of heat into acoustic energy.
In general, the medium is considered a premixed gas of reactants, which is ignited at some point in the domain, so that the combustion will raise the temperature downstream of the combustion zone. The combustion process itself is not taken into account. It is assumed that the unburnt and burnt gas both behaves as perfect gases, and that no molecular weight change occurs in the combustion process. If the combustion process were to be included more carefully, a model describing the chemical reaction along with evolution equations for the gas components would be needed. Here, the combustion is treated as kind of black-box process, the only outcome being heat addition and its consequences.

A portion of the gas in thermodynamic equilibrium will not have its temperature affected be the passing through of a sound wave i.e. a compression wave. This means that the compression acts as an adiabatic process, so that the entropy

remains constant (no entropy fluctuation). Which is why the acoustic field generally is considered isentropic.
Contrary, an unsteady heat release will cause temperature fluctuations unrelated to the pressure wave, which are convected by the flow. Therefore downstream of the flame there will also be an entropy waves present in the system, which is the mentioned convective wave with speed $\bar{u}$ in the Euler equations in non-conservative form. These entropy fluctuations will appear in the density fluctuation, which can have different effects.

The energy equation would be the most natural place to consider the heat release, since it is an energy source.
However, the path towards inclusion of the heat release source term presented below is the same as in [1]. This derivation is chosen, because it is based on thermodynamic considerations rather than just adding an energy source, and more clearly presents the deviation from the usual assumption of isentropicity in acoustics.
The heat input will affect the thermodynamics of the gas, so if the density is considered a state function of both pressure and entropy $\rho = \rho(p, s)$, the chain rule will give

$$\frac{\mathrm{D}\rho}{\mathrm{D}t} = \frac{1}{c^2}\frac{\mathrm{D}p}{\mathrm{D}t} + \left.\frac{\partial\rho}{\partial s}\right|_p \frac{\mathrm{D}s}{\mathrm{D}t} \tag{2.28}$$

since $\partial\rho/\partial p|_s = 1/c^2$.
Since the gas is considered inviscid and non heat-conducting, the change in entropy is given by the second law of thermodynamics

$$\rho T\frac{\mathrm{D}s}{\mathrm{D}t} = q(x,t) \tag{2.29}$$

where $q(x,t)$ is the heat input per unit volume.
The gas is considered perfect, hence $\partial\rho/\partial s|_p = -\rho/c_p = -\rho T(\gamma-1)/c^2$, and the expression (2.28) results in

$$\frac{\mathrm{D}\rho}{\mathrm{D}t} = \frac{1}{c^2}\left(\frac{\mathrm{D}p}{\mathrm{D}t} - (\gamma-1)q\right) \quad . \tag{2.30}$$

Combined with the continuity equation (2.1), this results in a evolution operator on the pressure similar to the previous derived expression (2.15c), but now with the sought source term caused by the heat release

$$\frac{\partial p}{\partial t} + u\frac{\partial p}{\partial x} + \gamma p\frac{\partial u}{\partial x} = (\gamma-1)q \quad . \tag{2.31}$$

This heat release is considered the cause of temperature changes in the medium. So a change in the stationary temperature field is the consequence of a stationary

heat release, which changes the properties of the medium but does not act as a source of sound.

However, if the heat release has an unsteady component, this will in turn act as an acoustic source. So when the heat input enters the linearized equations, the source term will consist of the unsteady part, while the steady part is entered implicitly through the mean values.

When the axial extent d of the combustion zone is very small compared to the acoustic wavelength – i.e. $kd \ll 1$, k being the wavenumber $\omega/\bar{c}$ – it is said to be acoustical compact. Thus this energy source can be viewed as a source onto a plane, represented by a Dirac δ-function. Although the stationary heat release could be distributed, the unsteady part is only considered non-zero at the flame position. If distributed steady heat release is part of the model, one would have to consider the conservation laws across this distribution. But here, the general expression used for the heat release is

$$q(x,t) = \big(\bar{q}(x) + q'(x,t)\big)\delta(x-\beta) \tag{2.32}$$

where $x = \beta$ is the position of the flame. The steady heat release $\bar{q}$ hence is discontinuous at the flame position, reflecting a sudden temperature change. If isothermal walls are considered, the steady heat release represents the energy necessary to divide the domain up- and downstream of $x = \beta$, into regions with different but uniform mean flow values. If losses due to cooling by the duct walls was included, this could be modelled by a smoothly varying steady heat release downstream of the combustion zone. A schematic representation of the model and the notations used is presented in Figure 2.1.

Note that the use of compactness is based on the acoustical wavelength, so in terms of the sound field it is well-founded. But the convective wave has a wavelength dependent on the mean flow velocity, and for low Mach number, the assumption of compactness $\omega d/\bar{u} \ll 1$ for the entropy wave is valid for very very low frequencies.

When the source enters the system, mathematical and numerical, it does so through balance of fluxes across the source, and as such on assumption of compactness. The entropy wave can have a strong influence on the acoustics under certain circumstances, and as such this lack of compactness is a factor that should be considered, since it might affect the numerical simulations.

The steady heat release changes the temperature, which in turn changes the properties of the gas regarding sound propagation. The characteristic impedance of the medium has a jump at the flame position, which causes an incoming sound wave to be partially transmitted and reflected. Considering the mass and momentum equation in a small volume around the impedance jump, it can be seen that the jump in pressure and velocity perturbations vanishes, as one could expect.

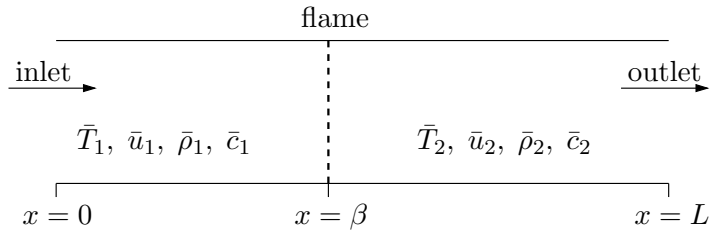

Figure 2.1: Scenario of the model set-up.

Also, the mean flow velocity changes across the heat release (by conservation of mass), so that all in all, the acoustic modes are affected by such temperature inhomogeneity.

The term thermoacoustic oscillation is related to the general scenario when heat exchange occurs in physics, i.e. the inhomogeneity of the medium caused by (steady) heat exchange and an eventual unsteady heat release. A heat release perturbation will locally cause volumetric expansion, acting as an acoustic monopole source.
Whenever there exists an coupling between the unsteady heat input and the acoustic field in the resonator, it is possible that this leads to the generation of self-sustained high amplitude oscillations in the chamber, the so-called thermoacoustic instability.

A coupling implies that the unsteady heat release is affected by the acoustic perturbations though the combustion zone somehow. If for example, the combustion process depends on the mass-flux fluctuation ($\rho'\bar{u} + \bar{\rho}u'$) – which could represent a premixed gas where the "supply" of reactants into the combustion zone is proportional to the acoustic field – then a higher sound level gives a higher (unsteady) heat release, giving more power to the acoustic field, increases the heat release, etc. This coupling is what can cause the acoustic instability, it acts as a positive feed-back mechanism. Or where it inverse proportional to an acoustic perturbation, it might lead to flame extinction, but this is not considered here.

A condition implying stability is the Rayleigh criterion. This states that when the pressure fluctuations and the unsteady heating are in phase, the acoustic mode will turn unstable. The criterion is given as

$$\int_0^T q'(t)p'(t)\ \mathrm{d}t > 0 \tag{2.33}$$

where T is the period of the oscillation. This criterion being satisfying might not be sufficient to guarantee stability, since also the interaction between the entropy wave and boundaries can lead to thermoacoustic instabilities ([1], [4]).

Modelling the combustion reaction can be a tricky affair, and many different suggestion can be found in the literature. This often involves combustion chemistry, with the medium composition and more complex combustion reaction expressions. In this project, the unsteady heat release model serves the purpose of creating the coupling and thus amplifying the resonant modes in the chamber, i.e. as the phase-locking mechanism so that the fundamental modes are the most dominant. The flame model primarily used here is that of the reference solution, since it is against this that the varying factors are compared and the method evaluated.

Balance conditions

Consider the source term the equation (2.31) and let this be represented by a delta function $q(x) = q(x)(x - \beta)$, so that the solution is discontinuous across the source position. Hence the equation are not valid across the source, since the solution is not continuous nor differentiable across the source. But this is not of great concern, since a weak solution is sought. So instead, the physical principles are supposed to hold, by requiring the flux of basic conservation quantities, expressed in integral formulation (or equivalently, a weak formulation), to be conserved or balanced in the limit over the source position. These are the Rankine-Hugoniot conditions across this imposed, stationary shock. For the heat release, this reads

$$[\rho u]_{\beta^-}^{\beta^+} = 0 \tag{2.34a}$$

$$[\rho u u + p]_{\beta^-}^{\beta^+} = 0 \tag{2.34b}$$

$$\big[u\big(\rho E + p\big)\big]_{\beta^-}^{\beta^+} = q \tag{2.34c}$$

where the factor $(\gamma - 1)$ has been dropped with respect to (2.31). When dealing with gas dynamics, these conditions tells something about the state on either side of a shock and here they express the differences in fluxes caused by a source term.

The energy balance (2.34c) tells us something about the scale of the heat release. The model has the temperature as a tunable parameter, so it would be natural to look at the total enthalpy density flux $\rho u(e + p/\rho + u^2/2)$. For a perfect gas, this gives

$$u\big(\rho E + p\big) = \rho u\big(c_P T + \tfrac{1}{2}u^2\big) \tag{2.35}$$

so it is a bit intuitive to take $\bar{q} \propto \bar{\rho}_1 \bar{u}_1 \big(c_P\big(\bar{T}_2 - \bar{T}_1\big) + \frac{1}{2}\big(\bar{u}_2^2 - \bar{u}_1^2\big)\big)$ considering in/out of the combustion zone.

The governing equations for the acoustics are linearized, so the Rankine-Hugoniot conditions above is not used as presented, but in a linearized form. The steady-unsteady splitting is introduced in these expressions (2.34), and the steady state form of the conditions is subtracted, again by the steady field implicitly having conservation of mass and momentum, and balanced energy, for the heat release. These RH-conditions for acoustic perturbations are presented here, and their use is described in later section on the numerical scheme.

$$\left[\rho'\bar{u} + \bar{\rho}u'\right]_{\beta^-}^{\beta^+} = 0 \tag{2.36a}$$

$$\left[p' + \rho'\bar{u}^2 + 2\bar{\rho}\bar{u}u'\right]_{\beta^-}^{\beta^+} = 0 \tag{2.36b}$$

$$\left[\left(c_{\scriptscriptstyle P}\bar{T} + \tfrac{1}{2}\bar{u}^2\right)\left(\rho'\bar{u} + \bar{\rho}u'\right) + \bar{\rho}\bar{u}\left(c_{\scriptscriptstyle P}T' + \bar{u}u'\right)\right]_{\beta^-}^{\beta^+} = q' \tag{2.36c}$$

The energy flux can also be describes in term of the used dependent variables. Either by the reformulation $u\big(\rho E + p\big) = \big(\frac{\gamma}{\gamma-1}pu + \frac{1}{2}\rho u^3\big)$ and linearizing, or equivalently by use of (2.36c) and the relation $c_{\scriptscriptstyle P}T' = p'/\bar{\rho} + \bar{T}s'$ and $c_{\scriptscriptstyle P}\bar{T} = \gamma\bar{p}/\bar{\rho}(\gamma-1)$. This results in the equation

$$\left[\frac{\gamma}{\gamma-1}\left(\bar{u}p' + \bar{p}u'\right) + \bar{u}^2\left(\tfrac{1}{2}\bar{u}\rho' + \tfrac{3}{2}\bar{\rho}u'\right)\right]_{x^-}^{x^+} = q' \tag{2.37}$$

which also is the used form in the implementation. The case of a stagnant medium (i.e. no flow) is also considered. The RH-conditions on the conserved quantities are not directly applicable in this case. The jump conditions, when the medium is at rest reduces significantly (see [1] for derivation), such that for unsteady heat release, the conditions becomes

$$[p']_{x^-}^{x^+} = 0 \quad \text{and} \quad [u']_{x^-}^{x^+} = \frac{(\gamma-1)}{\bar{\rho}_1\bar{c}_1^2}q' \qquad . \tag{2.38}$$

These jump conditions hence describes the coupling between the variables across a source, which is how they are used when a numerical model of the problem is constructed. As mentioned, the unsteady heat release is a sound source through volumetric expansion, and as such, the jump in primitive variables are expected to be largest (relatively) in the density fluctuations.
When a mean flow is present, the density fluctuation downstream of the point of application of these conditions will carry an "excess density" (deviation from $\rho' - p'/\bar{c}^2$), which is the entropy wave.

Driving sources

As mentioned, the unsteady heat release acts as an acoustic source, but only in presence of an acoustic field by the coupling of these. So there is need for an

extra source in order to generate the sound field.

Maybe the most simple way to generate an acoustic perturbation in the chamber is to let an inflow boundary condition (at $x = x_{\text{IN}}$) act as an abstraction of a piston, still allowing a mean flow to pass through i.e. an inlet boundary condition on the form $u(x_{\text{IN}}, t) = \bar{u}(x_{\text{IN}}) + u_0 e^{-i\omega t}$ with ω being the frequency and u_0 the amplitude of this acoustic perturbation.

In this project, again, the specific type of boundary condition is important for the resonator and it seemed reasonable not to start mixing a driver signal and the more physical boundary conditions. It might even deteriote the simulation, since incoming waves would "feel" the piston as well.

A modification of this approach, still in order to generate an acoustic field, is to use the hyperbolicity of the system, decomposing the system into its characteristics, and then imposing the driving source as the incoming wave and letting the outgoing passing through. If the model had non-reflecting boundaries as a requirement, this method would be more appropriate.

The inclusion of driving sources is done by adding source terms to either the mass or momentum conservation equation, which corresponds[1] to either externally mass-injection or force representation ([3, p. 28]). So for an external mass-injection, the inhomogeneous conservation law becomes

$$\frac{\partial \rho}{\partial t} + \frac{\partial}{\partial x}(\rho u) = \frac{\partial \rho f_\rho}{\partial t} \tag{2.39}$$

where the right hand side is the rate of injected mass by volume fraction f_ρ. And for an external force source per unit volume

$$\frac{\partial}{\partial t}(\rho u) + \frac{\partial}{\partial x}(\rho u u + p) = f_u \tag{2.40}$$

These two sources are fixed in space and considered compact (δ-sources), and are used to drive the system with a broadband signal. The exact expression of this signal is given later.
During the linearization process, the momentum source does not change (and hence is considered small-scale), while the mass-injection term results in $\bar{\rho}\, df_\rho/dt$, again with f_ρ being small.

The inclusion of a mass term in (2.39) affects the formulation of the momentum conservation in non-conservative form (2.15b) by adding a term $-u\partial(\rho f_\rho)/\partial t$ or in linearized form $-\bar{u}\bar{\rho}\partial f_\rho/\partial t$. However, when the source is included in the numerical scheme, it enters through considerations about the conservative form of the system. So the term does not matter as such, and is ignored here.

[1] these are simplifications, the actual physical process can be rather complicated

Either one of these source terms can be applied through the appropriate jump conditions (2.36a) or (2.36b), and be included into the numerical method in the same way as the unsteady heat release, as will be explained later.

By considering the conservation laws (2.39) and (2.40) in a integral formulation, one can arrive at more simple jump conditions/estimates for such external sources [3, p.84]. For the mass injection at instant time this reads

$$[u']_-^+ = f_\rho \quad \text{and} \quad [\rho']_-^+ = [p']_-^+ = 0 \tag{2.41}$$

with the superscripts $\pm$ denoting either side of the source position. Very similar, the jumps describing an external force are

$$[p']_-^+ = f_u \quad \text{and} \quad [u']_-^+ = [\rho']_-^+ = 0 \qquad . \tag{2.42}$$

The jump expression (2.41) is used in stagnant medium to represent a mounted loud-speaker with some volume velocity f_ρ, and when an isentropic model with mean flow is considered (presented in later section), these are the conditions used to enter the driver in the numerical scheme.
The signal used to drive the chamber is considered in greater detail in the following section

The placement of the acoustic drivers for the stagnant medium is not important, this just creates an acoustic disturbance. But when there is a flow, the placement matters. The driver is imposed via jump conditions, so the solution is discontinuous across the driver. This discontinuity creates entropy fluctuations since entropy cannot be conserved across a shock. This entropy fluctuation convects with the flow, so this has to taken into account if the model expects that the acoustic wave entering the combustion zone is isentropic. Placing the driver downstream of the heat release source removes this particular problem with respect to the heat source.

Some of the forms for including a driver source generates stronger entropy waves than others. The simple velocity jump condition (2.41) generates only weaker entropy waves. Hence, if outlet boundary conditions would have an effect by the impinging entropy wave, it would be more appropriate to use the simpler (2.41) in order not to add to this boundary effect unnecessarily..

Driving signal

The reason for solving this acoustic problem in the time-domain, relies on its non-restriction (in regard of formulation) to single frequency perturbations. So the idea is to excite the chamber with a signal which covers some frequency band,

so that the unknown, and possibly more, resonance frequencies are excited. A linear broadband signal is chosen here. In principle, a block signal (or binary signal) would have a broader spectrum, but the propagation of such a signal is more complex in regard of the numerical treatment. Besides, it is expected that the different conditions under consideration, will shift the fundamental, geometric eigenfrequency, but not with large jumps. So the excitation spectrum can be set thereafter, and a signal with a relatively narrow spectrum would still excite the sought instability frequencies, and give, in the end of the process, spectras just as good. So occam's razor applies, and the simpler, linear driving signal is used.
The expression for the driver signal, also known as a sweep signal, is given as

$$y(t) = A \sin\big((\Delta\omega\, t + \omega_{\min})\, t\big) \tag{2.43}$$

where $\Delta\omega = 2\pi(f_{\max} - f_{\min})$ is the interval of angular frequency and $\omega_{\min}$ the lower frequency. The amplitude is set to the scale of the acoustic perturbations. This signal is used over intervals of $1s$, so the simulations are usually run over this time-interval. In Figure 2.2 is shown an example of such a sweep signal.

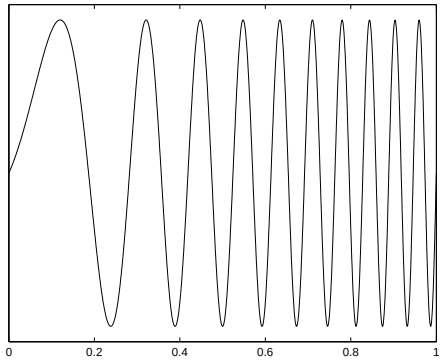

Figure 2.2: Sweep signal example, $f \in [0, 10]$.

2.5 Elaboration on the different considerations

The reason for the definition of the numerical experiments is twofold. One is to set up some different considerations that could have an acoustical effect and use the numerical simulations to investigate this. And secondly, to have some different perspective regarding the numerical method itself. The subject of comparison are thus chosen as to describe not too different model set up in regard of physics, in order to see how this influences both the sound field itself and the simulation of it.

In terms of the acoustics, the question is, does some assumptions or aspects in regard of the model affect the system in terms of possible resonant modes, and if this is the case, how much. Or can a simpler model be used without losing the effects of whatever phenomenon is taking place or can an deviation be predicted and "corrected" for.

Here, the two assumption in question, are the constant mean pressure assumption although a temperature change being present, and the very general assumption of an isentropic medium.

The combustion that takes place might raise the gas temperature significantly, and that this change in temperature should solely be balanced by density change even in the low Mach limit, is less likely. This is a question that is related to the (given) stationary flow values in the model and especially related to modelling the stationary heat release.

The assumption of isentropicity is related to the fluctuating quantities. The unsteady heat release can cause convected temperature perturbations not associated with the pressure fluctuations (the entropy waves) which can have an effect on the resulting sound field. This is thought to have an effect for low frequencies only.
So this "versus"-case is meant to indicate whether the full system of equations should be used or if a reduced (appropriate) model is satisfactory.

2.5.1 Constant Mean Pressure

Although the differential equations are invalid across the flame position, the conservation laws still tells something about the inter-dependency of the steady state values. And if the mean velocity change, so should the mean pressure.

A constant mean pressure is sometimes assumed for small temperature gradient in a relatively narrow geometry. Here the temperature changes abruptly, and

one might imagine that on the path towards equilibrium of the gas across the heat source, would be an isobaric process.
Also an argument for the constant mean pressure is due to the low Mach number. This can be seen by considering the momentum equation in conservative form for steady state values,

$$\bar{\rho}\bar{u}\bar{u} + \bar{p} = \text{constant} \tag{2.44}$$

which can be rewritten as

$$\bar{p}\left(1 + \gamma M^2\right) = \text{constant} \tag{2.45}$$

since a perfect gas has the relation $\bar{\rho}\bar{c}^2 = \gamma\bar{p}$. When the Mach number is small ($\ll 1$), one could argue that mean pressure should be constant.

When the medium is stagnant, there will be no mean pressure gradient. So when the mean pressure is constant across the initial temperature raise, the change in temperature would have to be counter-acted by density change, by the equation of state for the gas, i.e. $\bar{p} = \bar{\rho}_1 R\bar{T}_1 \;\Rightarrow\; \bar{\rho}_2 = \bar{p}/R\bar{T}_2$ where the suffices refers to the states on either side of the combustion zone.
When there is a low-speed flow and the same assumption of constant pressure is used, the temperature change also affects the mean flow. Continuity requires that $\bar{\rho}\bar{u}$ is constant, so the mean velocity downstream is given as $\bar{u}_2 = \bar{\rho}_1\bar{u}_1/\bar{\rho}_2$. So, obviously, the larger the temperature difference across the heat source, the greater jump in density, velocity etc. for constant pressure. Hence this approach would not be appropriate if very large temperature jumps is uses as data.

Contrary to this view, the mean flow values are affected by the heat release with a change in mean pressure. The mean flow values downstream of the heat source are found by representing the steady heat release as the total enthalpy density flux, i.e. as mentioned previously

$$\bar{q} = \bar{\rho}_1\bar{u}_1\Big(c_P\big(\bar{T}_2 - \bar{T}_1\big) + \tfrac{1}{2}\big(\bar{u}_2^2 - \bar{u}_1^2\big)\Big) \qquad . \tag{2.46}$$

The equations describing the downstream values are the conservation laws in integral form across the source, i.e.

$$\bar{\rho}_2\bar{u}_2 = \bar{\rho}_1\bar{u}_1 \tag{2.47}$$

$$\bar{p}_2 + \bar{\rho}_2\bar{u}_2^2 = \bar{p}_1 + \bar{\rho}_1\bar{u}_1^2 \tag{2.48}$$

$$\frac{\gamma}{\gamma-1}\bar{p}_2\bar{u}_2 + \tfrac{1}{2}\bar{\rho}_2\bar{u}_2^3 = \bar{\rho}_1\bar{u}_2\Big(c_P\big(\bar{T}_2 - \bar{T}_1\big) + \tfrac{1}{2}\big(\bar{u}_2^2 - \bar{u}_1^2\big)\Big) \tag{2.49}$$

$$+ \frac{\gamma}{\gamma-1}\bar{p}_1\bar{u}_1 + \tfrac{1}{2}\bar{\rho}_1\bar{u}_1^3 \tag{2.50}$$

by which the values $\bar{\rho}_2$, $\bar{u}_2$ and $\bar{p}_2$ are found though Newton iteration.
For the compact heat source used here, this method provides consistent mean

flow values, although one could question the use of an enthalpy jump for the heat release for larger temperature change, since the change in pressure becomes significant

In Figure 2.3 is show the difference in resulting medium properties downstream of the temperature change. The deviations are presented as the difference between the value for constant pressure and pressure drop, relative to the upstream value, e.g. for the pressure $\left(\bar{p}_{2,\mathrm{Const}} - \bar{p}_{2,\mathrm{Drop}}\right)/\bar{p}_1$. The deviations are signed, thus the positive deviation in pressure cases and likewise in the other variables. It is seen that the downstream speed of sound is more or less unaf-

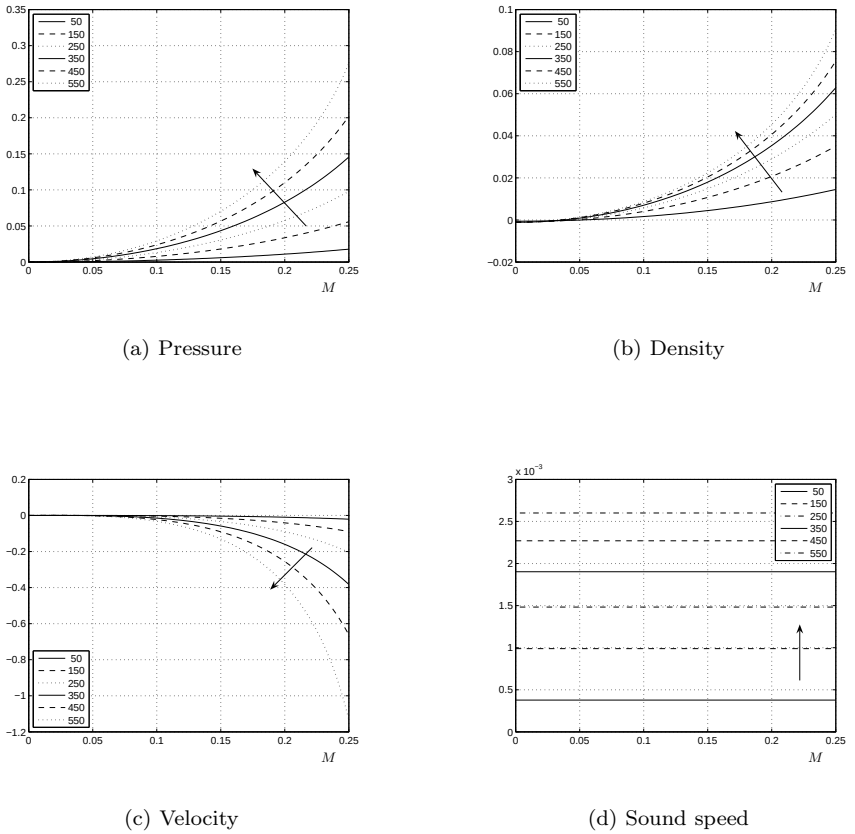

(a) Pressure

(b) Density

(c) Velocity

(d) Sound speed

Figure 2.3: Relative deviation in mean flow between $\left(\bar{q}_{2,\mathrm{Const}} - \bar{q}_{2,\mathrm{Drop}}\right)/\bar{q}_1$ across heat the heat release by (2.46). Arrows shows increasing temperature with $\bar{T}_2 - \bar{T}_1$ in the legends. .

fected by the flow velocity, and that the change in pressure is counteracted by

density change, with respect to the resulting sound speed. And that the mean velocity is significantly higher for the pressure drop case, at large temperature jumps and higher inlet velocity.

Based on this, and since the comparison is meant for low-speed mean flow, the upper mean velocity limit is taken so that $0 \leq M_1 \leq 0.15$, otherwise the mean velocity downstream differs to considerably for the used temperature changes.

2.5.2 Isentropicity

What if we can formulate the problem, such that no entropy wave can be present, but still considers the acoustic source effect of the heat release.

Over the flame, isentropicity can not be assumed, but it does not matter, since here other equations (the Rankine-Hugoniot conditions) describes the behavior of the gas. So the above system in a linearized form is used on either side of the heat release, such that no entropy wave should be present downstream of the heat source, but the unsteady heat still acting as a source of sound

The entropy wave/mode is carried by the density fluctuation, and can generate acoustic perturbations by a coupling between boundaries and the presence of these temperature fluctuations. For instance a choked outlet can give pressure reflections. Here the outlet is an open end, which just convects the entropy wave. So it is the effect of its presence (or "allowed" presence) that is questioned for a certain case of physical setup.

The isentropicity starts with $\mathrm{d}s = 0$, or in term of total derivative

$$\frac{\mathrm{D}s}{\mathrm{D}t} = 0 \tag{2.51}$$

This is a general form of the energy conservation equation when a non-heat conducting and inviscid medium is considered. In view of (2.28), this gives the often used equation of state for isentropic flow

$$\frac{\mathrm{D}p}{\mathrm{D}t} = c^2 \frac{\mathrm{D}\rho}{\mathrm{D}t} \tag{2.52}$$

in deriving the equations of linear acoustics. If (2.51) has to hold with no entropy fluctuations, the flow has to be homentropic as well i.e. $\bar{s}$ is constant. So the temperature is considered uniform on either side of the heat release.

The isentropic version of the Euler equations in nonconservative form can be reduced to the momentum equation and – using the energy equation as (2.52) and the mass conservation equation (2.1) to eliminate for ρ – an equation for

the pressure evolution. These are of course the same used previously, repeated here for convenience.

$$\frac{\partial u}{\partial t} + u\frac{\partial u}{\partial x} + \frac{1}{\rho}\frac{\partial p}{\partial x} = 0 \tag{2.15b}$$

$$\frac{\partial p}{\partial t} + u\frac{\partial p}{\partial x} + \gamma p\frac{\partial u}{\partial x} = 0 \tag{2.15c}$$

These two equations are usually used to linearize and form the acoustic wave equation. Under the simplifying assumptions of no mean flow gradient and homogeneous medium, the acoustics are described by the modified wave equation

$$\frac{\partial^2 p'}{\partial t^2} + \left(\bar{u}^2 - \bar{c}^2\right)\frac{\partial^2 p'}{\partial x^2} + 2\bar{u}\frac{\partial^2 p'}{\partial t \partial x} = 0 \tag{2.53}$$

Through reducing the system order by explicitly expressing isentropicity, we see that the solution, in term of invariants/characteristic waves/ travelling waves, now only consist of two waves, travelling at speed $\bar{u} \pm \bar{c}$.

Previously, when the entropy wave was considered present in the solution, this could not be seen directly from the governing equations, since neither temperature fluctuations nor entropy fluctuations occurred in the equations as such. Nevertheless, the entropy wave was considered there and carried in the density fluctuation through convection. It was the characteristic travelling at mean flow speed.
The unsteady temperature caused by unsteady heat release, enters through the Rankine-Hugoniot conditions for the acoustic perturbations, and it is through the coupling here, that the entropy wave starts and is convected. Even if isentropicity is assumed everywhere, it can not be assumed across the heat source, and if the equations allow for the wave to exists, it will "propagate" by convection.

Now, we consider equations which do not allow for entropy waves as such, the system being reduced. But the RH conditions were imposed in order to respect the conservation laws, and as such should still apply when the heat source is there. The source is still sought included in the same way as described previously, so there is one equation to many, since when included in the numerical scheme, the number of equations needed is the number of dependent variables.

This is overcome by using the RH conditions for the acoustic fluctuation (2.36), by eliminating for the downstream density fluctuation and using the fluctuating mass flux condition. This provides the two equations

$$p_2' + \bar{\rho}_2\bar{u}_2u_2' - p_1' - \rho_1'\bar{u}_1(\bar{u}_1 - \bar{u}_2) - \bar{\rho}_1(2\bar{u}_1 - \bar{u}_2)u_1' = 0 \tag{2.54a}$$

$$\frac{\gamma}{\gamma-1}\left(\bar{u}_2p_2' + \bar{p}_2u_2'\right) - \frac{\gamma}{\gamma-1}\left(\bar{u}_1p_1' + \bar{p}_1u_1'\right) + \bar{\rho}_1\bar{u}_1\bar{u}_2u_2' - \bar{\rho}_1\bar{u}_1^2u_1' - (\rho_1'\bar{u}_1 + \bar{\rho}_1u_1')\frac{1}{2}\left(\bar{u}_1^2 - \bar{u}_2^2\right) = (\gamma-1)q' \tag{2.54b}$$

The density fluctuation immediately upstream of the source is present in the equations, but the sound field here is assumed isentropic with isentropic boundary conditions, so it is tempting to take $\rho_1' = p_1'/\bar{c}_1^2$, so these equations solely are described by p' and u'.

This case is meant to investigate if the reduced system along with the above conditions gives the same acoustic behavior when simulated. Naturally, this only applies for some specific cases of model. It would, for example, be rather difficult to express non-isentropic boundary conditions with such a reduced system.

Chapter 3

Discontinuous Galerkin Method

In this chapter is presented used numerical method, the discontinuous Galerkin method.
The discontinuous Galerkin method can be seen as a hybrid method between the finite element and the finite volume method. It shares the geometric flexibility of both the FEM and FVM in regard to unstructured meshes, and has the conservation properties of the FVM and the higher-order property of FEM. It has been applied to a large variety of problems now, and is generally considered to be quite flexible.

The MATLAB codes used in this project are based on codes presented in [2], and how all the necessary parts of the scheme are set up, will not be a subject in the following. The principles of the method will be presented, with emphasis on the properties this particular scheme holds, and are "appropriate" for the model in regard.

The equations will be semi-discretized i.e. the spatial operators are to be approximated with the dG method, while the temporal integration is handled with some Runge-Kutta method.

In this chapter, the first couple of sections concern a very general description of the dG method. Then follows the details which are relevant to the problems in

this thesis. At last is the part regarding inclusion of sources.

Regarding notation, the style will be adapted from [2], since this book has served as textbook on the subject.

The model concerns 1D in space, so the presentation of the numerical scheme is restricted to the 1D case. By this in mind, the scheme is fully extendable to higher dimensions.

3.1 Discontinuous Galerkin Formulation

Consider the system (2.17), expressed as

$$\frac{\partial \boldsymbol{u}}{\partial t} + \frac{\partial A\boldsymbol{u}}{\partial x} + B\boldsymbol{u} = 0 \tag{3.1}$$

where $\boldsymbol{u} = (\rho', u', p')^T$ being the primitive variables. This is a system of coupled advection equations with constant matrices A and B, given as

$$A = \begin{bmatrix} \bar{u} & \bar{\rho} & 0 \\ 0 & \bar{u} & 1/\bar{\rho} \\ 0 & \gamma\bar{p} & \bar{u} \end{bmatrix} \quad , \quad B = \begin{bmatrix} 0 & 0 & 0 \\ \bar{u}\bar{u}_x/\bar{\rho} & 2\bar{u}_x & -\bar{\rho}_x/\bar{\rho}^2 \\ 0 & (1+\gamma)\bar{p}_x & (1+\gamma)\bar{u}_x \end{bmatrix} \tag{3.2}$$

where the matrix $B \equiv 0$, if the mean flow is uniform on either side of the heat source. In the following presentation, such a uniform flow is assumed, because it corresponds to the main situation in the acoustic model, and because it does not have change the derivation of the numerical scheme. Hence, the equation (3.1) is presented in a general conservation form

$$\frac{\partial \boldsymbol{u}}{\partial t} + \frac{\partial \boldsymbol{f}(\boldsymbol{u})}{\partial x} = 0 \tag{3.3}$$

with $\boldsymbol{f}(\boldsymbol{u}) = A\boldsymbol{u}$

In the following presentation of the scheme, the equation to be discretized is a scalar equation. This is only to make the notation easier, it is directly applicable on each equation in the system (3.3).

So the problem equation is

$$\frac{\partial u}{\partial t} + \frac{\partial f(u)}{\partial x} = 0 \tag{3.4}$$

along with some initial condition $u(x, 0) = u_0(x)$ and boundary conditions.

The solution is sought in the spatial domain $\Omega : x \in [0, L]$, initially by a finite element formulation. The finite element formulation consists of dividing the spatial domain in non-overlapping and not necessarily uniform elements $D^k = \left[x_-^k, x_+^k\right]$, such that $\Omega = \bigcup_{k=1}^{K} D^k$, and expressing the solution u on each element as a local polynomial approximation u_h^k. The N'th order polynomial representation can be either on a modal or a nodal basis, such that the local element-wise solution for $x \in D^k$ is represented as

$$u_h^k(x,t) = \sum_{n=0}^{N} \hat{u}_n^k(t)\psi_n(x) = \sum_{i=0}^{N} u_h^k(x_i^k,t)l_i(x) \tag{3.5}$$

where the $\hat{u}_n^k$ are the modal expansion coefficients, while the $u_h^k(x_i^k,t)$ are the nodal values. The basis considered here, of which different choices could be made, are the Legendre polynomials ψ_n and the Lagrange interpolating polynomials $l_i(x)$. The order of the approximation is one of the parameters to control the discretization error, the other being the number of elements covering the domain. This polynomial approximation is what gives the scheme the nice property of having spectral convergence, i.e. for polynomial projections and smooth solutions $u \in H^p$ with p large – which denotes solutions with $p-1$ continuous derivatives and bounded p'th derivative – the approximation error $\|u - u_h\|$ is $\mathcal{O}(N^{-p})$, which is a very fast convergence.

The solution to the equation is then the sum of these local solutions

$$u(x,t) \approx u_h(x,t) = \sum_{k=1}^{K} u_h^k(x,t) \qquad . \tag{3.6}$$

The "approximation error" by this polynomial representation is the quantity, that is wanted minimized, or more precisely, wanted to be a zero-function, in the weak sense of a L^2-norm (the inner product). This is done by expressing a residual $R(u_h)$ by the polynomial approximation inserted into the equation, then multiplying with a test function ϕ, locally defined on each element and continuous on this, and then taking the inner product. In the Galerkin framework, these test functions are chosen from the same function space as the one used to express the polynomial approximation (the trial functions).
So on each element, the problem is defined as

$$\forall k,l \qquad \int_{D^k} R(u_h^k)\phi_l(x)\,\mathrm{d}x = \int_{D^k} \left(\frac{\partial u_h^k}{\partial t} + \frac{\partial f_h(u_h^k)}{\partial x} \right) \phi_l(x)\,\mathrm{d}x = 0 \tag{3.7}$$

where

$$u_h^k = \sum_{n=0}^{N} \hat{u}_n^k(t)\phi_n(x) \tag{3.8}$$

is a general representation used henceforth, where the test function ϕ could be either the Legendre basis functions ψ or the Lagrange basis l, as given in (3.5).

Performing integration by parts on the spatial derivative once, gives the weak form of the scheme

$$\forall k, l \qquad \int_{D^k} \left(\frac{\partial u_h^k}{\partial t} \phi_l - f(u_h^k) \frac{d\phi_l}{dx} \right) \, \mathrm{d}x = - \left[f^* \phi_l \right]_{x_-^k}^{x_+^k} \tag{3.9}$$

The flux evaluation at the element edge $f(u_h^k)\big|_{\partial D^k}$ is the place where the dG-method separates itself from the finite element formulation. In the finite element formulation, the basis usually vanishes at element edges, such that the right hand side in (3.9) is zero.

Since the trial space, onto which the numerical solution is decomposed, has no requirement of continuity across elements, this flux can be multiply defined as both $f(u_h(x_+^k, t))$ and $f(u_h(x_-^{k+1}, t))$, since $x_+^k = x_-^{k+1}$. This ambiguity is the reason for introducing the so-called *numerical flux* or *trace* f^* in (3.9), which is a key concept in the dG-method. How this is defined and what function it serves, will be adressed later. But from the above expression it is apparent, that something having to do with an element edge, comes into the scheme by this numerical flux.

This deficiency of continuity requirement in-between elements is also a reason why the dG method has efficiency advantages. The elements decouple in a sense, so that for large problems (in terms of grid), each element can be solved for, on its own i.e. the scheme is parallizable, a valuable property when dealing with large time-dependent problems.

The dG scheme has a second form, called the strong form, which results from the weak form (3.9) by re-doing integration by parts

$$\forall k, l \qquad \int_{D^k} \left(\frac{\partial u_h^k}{\partial t} + \frac{\partial f(u_h^k)}{\partial x} \right) \phi_l \, \mathrm{d}x = \left[\left(f(u_h^k) - f^* \right) \phi_l \right]_{x_-^k}^{x_+^k} \tag{3.10}$$

These two forms are mathematically the same, although the strong form should have a tendency of better convergence. Also it is the form used in the implementation, although no difference was found between using the weak and the strong form.

Inserting the polynomial representation (3.8), and of course a similar representation of the flux function, into the weak form (3.9), and interchanging summation and integration yields for each element

$$\sum_{n=0}^{N} \frac{\partial \hat{u}_n^k}{\partial t} \int_{D^k} \phi_n \phi_k \, \mathrm{d}x - \sum_{n=0}^{N} \hat{f}_n^k \int_{D^k} \phi_n \frac{d\phi_k}{dx} \, \mathrm{d}x = - \left[f^* \phi_l \right]_{x_-^k}^{x_+^k} \tag{3.11}$$

or equivalently expressed in matrix-vector notation, with $\hat{\boldsymbol{u}}_h^k = \left(\hat{u}_0^k, \ldots, \hat{u}_N^k\right)^T$ being the vector of solution coefficients, and the same for $\hat{\boldsymbol{f}}_h^k$:

$$\mathrm{M}^k \frac{d\hat{\boldsymbol{u}}_h^k}{dt} - \left(\mathrm{S}^k\right)^T \hat{\boldsymbol{f}}_h^k = -\left[f^* \phi_l\right]_{x_-^k}^{x_+^k} \tag{3.12}$$

where the matrices are being defined as

$$\mathrm{M}_{ij}^k = \int_{D^k} \phi_i \phi_j \, \mathrm{d}x \quad , \quad \mathrm{S}_{ij}^k = \int_{D^k} \phi_i \frac{d\phi_j}{dx} \, \mathrm{d}x \tag{3.13}$$

The strong form results in a similar form, as

$$\mathrm{M}^k \frac{d\hat{\boldsymbol{u}}_h^k}{dt} + \mathrm{S}^k \hat{\boldsymbol{f}}_h^k = \left[\left(f(u_h^k) - f^*\right) \phi_l\right]_{x_-^k}^{x_+^k} \tag{3.14}$$

The matrices M^k and S^k are local operators, since they depends on the basis defined on each element and in principle should be defined for each element. Without going into details with the implementation, this is overcome by defining the basis on a reference element, such that these matrix operators operate on the reference element and then mapped onto the physical, spatial element. This is however more of an efficiency concern.
The independency of each element equation system – (3.9) or (3.10) – with respect to each other, adds the property of being *hp*-adaptive to the scheme. This means that adjacent local solutions can be approximated in different order and/or over elements of different lengths. So the grid spacing and approximation order can be adjusted to parts of the problem, if needed. This can also be done during the calculations, with an extra computational effort of course, so that parts of the solution can be discretized "at a smaller scale" or eventually tracked.

This above form are reduced even further, again without considering the details about construction etc. such that e.g. for the strong form

$$\frac{d\hat{\boldsymbol{u}}_h^k}{dt} + \mathrm{D}^k \hat{\boldsymbol{f}}_h^k = \left(\mathrm{M}^k\right)^{-1} \left[\left(f(u_h^k) - f^*\right) \phi_l\right]_{x_-^k}^{x_+^k} \tag{3.15}$$

where the matrix D^k acts as a differentiation matrix (or a interpolation form of the derivative), in much the same way as in spectral methods.

This is the sought semi-discretization of the PDE, now we can apply an integrator for the time-derivative, where the right hand side of this "ODE" is the spatial discretization, i.e.

$$\frac{d\boldsymbol{u}_h^k}{dt} = \boldsymbol{F}(\boldsymbol{u}_h^k, t) \tag{3.16}$$

$$\boldsymbol{F}(\boldsymbol{u}_h^k, t) = -\mathrm{D}^k \hat{\boldsymbol{f}}_h^k + \left(\mathrm{M}^k\right)^{-1} \left[\left(f(u_h^k) - f^*\right) \phi_l\right]_{x_-^k}^{x_+^k} \tag{3.17}$$

The integrator used is the 4'th order, 5 stage Low Storage Runge-Kutta method presented in [2]. Alternatives have been tried in form of a 4'th order, 6 stage Low Dispersion Low Dissipation Runge-Kutta (also in low storage form), but without distinct differences. So the cheaper 5 stage scheme was used.

The discretization in space sets a bound on the time-step, in a CFL-sense. The time-stepping should ensure that the domain of dependence (regarding the hyperbolicity of the problem) is respected. So a bound on time-step involves the minimum spatial discretization length, but it also has to take into account the speed of the propagating waves in the system. A bound can be formulated as ([2, p.62]),

$$\Delta t \leq C \frac{\min \Delta x}{\rho(A)} \tag{3.18}$$

with $\rho(A)$ being the (global) spectral radius of the flux coefficient matrix in (3.1). When frequency analysis is performed on recorded time-series, the time-step (or sampling rate) is small enough to guarantee that waves in the frequency range considered are represented.

3.2 Numerical flux

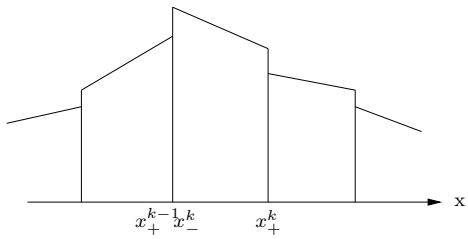

Figure 3.1: The ambiguity of values

The role of the numerical flux f^* is to supply a single value, where actually there are two, since the solution and test functions are allowed discontinuous across an element edge, as shown in Figure 3.1.

It is by the numerical flux that the element couples to adjacent elements, which means that for an element D^k, the flux at the left endpoint x_-^k should be a function of the local approximation value at x_-^k and the adjacent value x_+^{k-1} i.e. $f^* = f^*\left(u_h^k(x_-^k), u_h^{k-1}(x_+^{k-1})\right)$ and equivalently for the right endpoint.
With the standard notation, where superscript $^-$ refers to local value, while $^+$ refers to the neighbor, the numerical flux is expressed in general as $f^*(u^-, u^+)$.

This also means, that for boundary elements i.e. elements with edges coinciding with $\partial\Omega$, the boundary condition enters the scheme through the flux, where the condition is imposed weakly by setting the external value to an appropriate value e.g. for the left endpoint of the domain $f^* = f^*\left(u_h^1(x_-^1), u_{h,\mathrm{BC}}\right)$. To impose boundary conditions in this way seems a good way to treat "the imposing boundaries problem", since it is done the exact same way in the interior domain. No special treatment of the boundary conditions is required as such, which can be quite a challenge in some numerical schemes.

A proper choice of numerical flux is what ensures stability of the scheme. Stability of the scheme is analyzed by use of the energy method, a method that aims at proving a stability condition in the form $\|u_h(t)\|_\Omega \leq c(t^*), t \in [0, t^*]$. The details of this analysis can be found in [2, chap. 4], which also include consistency and convergence analysis. In brief, if the scheme is consistent and stable, convergence follows by the Lax equivalence theorem.

The choice of numerical flux, assuming that it renders the dG method stable, is somewhat arbitrary. The theory regarding the use of such fluxes stems from the finite volume method, since it is a crucial part of this numerical scheme.
In the finite volume method, cells (or control volumes) are considered, and the solution averaged over these cells[1]. At the interface between two such cells, a flux evaluation is needed.

When a homogeneous conservation law is considered, this can be expressed as a Riemann problem at the cell interface (a very simple description). Much work has been put into deriving exact and approximate Riemann solvers in the form of such numerical fluxes. Note that in the finite volume context, the choice of numerical flux is essential since it plays a major part in the scheme. In the dG context, the numerical flux is merely used to provide stability and connection between elements, by defining the intermediate flux between the local solutions. It is still a Riemann problem in this context, but an exact solution is much less necessary. So the computational complexity of the flux evaluation is also a factor to be taken into account.

The formulation of the numerical flux has to fulfill some basic properties, some more intuitive than others. It has to be consistent, so that $f(u_h) = f^*(u_h, u_h)$. And it has to be monotone, following results from the finite-volume theory. A monotone scheme is highly stable, and more important, recovers the correct physical solution in form of the entropy solution.

A simple and widely used flux is the Lax-Friedrich flux, defined as

$$f^{LF}(u^-, u^+) = \frac{f(u^-) + f(u^+)}{2} + \frac{C}{2}\left(u^- - u^+\right) \tag{3.19}$$

[1] when the polynomial approximation in the dG method is zero i.e. a constant representation, the two methods more or less coincide

where the constant C, which reflects the largest speed, is defined as

$$C \geq \max \left| \frac{\partial f}{\partial u} \right|_{\Omega} \tag{3.20}$$

or defined locally

$$C \geq \max \left| \frac{\partial f}{\partial u} \right|_{D^k} \tag{3.21}$$

When it is a system of equations, the constant C is chosen as the maximum eigenvalue of the flux Jacobian, which in this case is $\bar{u} + \bar{c}$, either globally or locally. The global constant results in a generally more dissipative flux.

Without the term $\frac{C}{2}(u^- - u^+)$, the flux is simply the average of the two fluxes, known as the central flux. The central flux is energy conserving.
Adding this extra term introduces artificial dissipation into the flux, proportional to the jump value, which is the stabilization mechanism of the scheme. Considering the strong form of the scheme (3.10), one sees that the flux jump has a connection with the residual integral over the element. Thus the higher an approximation within the element, the smaller the jump over element interfaces.

The local Lax-Friedrich (LLF) flux is the one used everywhere in the domain. The reason is that the scheme, in space and time, is used to let the resonance modes develop and propagate. For this, a flux which is cheap to calculate and stabilizes the scheme is sufficient, so the Lax-Friedrich (global or local) will work fine. If other problems were considered, e.g. the scattering effect of a jump in material properties, other flux formulations could be more appropriate.
A derived upwind flux was tried in order to see if this change of flux would affect the propagation through the material interface (where the medium changes its properties). This upwind flux is supposed to have an less dissipative effect at such discontinuous material properties, but with respect to the excited resonance frequencies, no difference was found.

What is more important in this context, is that the waves propagate at the correct phase, since in the numerical experiments, the spectras are used as data. When simulating acoustics, a "correct" wave propagation is a highly appreciated property of a numerical scheme. This requires the scheme to represent the dispersion relation of the solution well, or said otherwise the phase error introduced by the scheme should be minimal. In this regard, the dG method does well, the dispersion error behaves as $\mathcal{O}(\big(hk\big)^{2p+3})$ when waves are well resolved (h representing the spatial discretization and k the wavenumber). And this error is independent[2] of the choice of numerical flux.

[2]independent in the sense that this error is not affected much by different fluxes

3.3 Inclusion of sources

The equations presented so far have been without the source terms, and noting have been said about how to handle these terms.

These sources, whether it be the unsteady heat release or the drivers, are expressed as δ-functions, with the condition that some jump relation is balanced across the source. The one condition being inhomogeneous (depending on the source in regard) will cause a shock at this point and the solution is discontinuous. Since the dG method allows for discontinuous solutions across element interfaces, it is quite natural to place an element interface at the source location and imposing the source weakly through the numerical flux.

So, by the balance condition, the values of each dependent variable will have different values on each side of the interface, and therefore different fluxes. The approach taken in this project is to calculate the wanted states on either side of the interface, and then imposing this state as if it were the solution adjacent to the element.

The calculation of these wanted interface states should take into account the RH-constraints and also the present waves passing through the flame zone. So the idea is to set up a system of equation for the six unknowns (the three dependent variables on each side of the source) describing this. The three linearized RH-conditions gives half the required equations, and the rest is used to connect the unknowns states to the surrounding solution.

This is where the hyperbolicity comes in. Because of this property, we know that the solution consists of three waves, travelling at different speeds in different directions. And that these waves follows some characteristic lines along which they are constant.

The characteristic invariants are not constant across the sources though, where also the characteristic speeds jump across the heat source, by the medium inhomogeneity. But between the wanted state and the actual state on either side, we can demand the waves entering the wanted state, to be conserved, see Figure 3.2 for a schematic representation. So on either side the conditions are written in terms of these propagating directions i.e. two equations from the upstream side and one from the downstream.

The weak formulation for the solution and the known hyperbolicity provides a way to express the contribution to the wanted states, from the ingoing waves.

The characteristic form of the linearized Euler equations reads,

$$\begin{aligned}
\Big(\tfrac{1}{2}\big(\bar{\rho}\bar{c}u' - p'\big)\Big)_t + (\bar{u}-\bar{c})\Big(\tfrac{1}{2}\big(\bar{\rho}\bar{c}u' - p'\big)\Big)_x &= 0 \\
\big(\rho' - p'/\bar{c}^2\big)_t + \qquad \bar{u}\Big(\rho' - p'/\bar{c}^2\Big)_x &= 0 \\
\Big(\tfrac{1}{2}\big(\bar{\rho}\bar{c}u' + p'\big)\Big)_t + (\bar{u}+\bar{c})\Big(\tfrac{1}{2}\big(\bar{\rho}\bar{c}u' + p'\big)\Big)_x &= 0
\end{aligned} \tag{3.22}$$

While the solution is discontinuous across $x = \beta$, the incoming characteristic waves can be expected to be conserved between the actual state and the wanted state. Formulated in a weak sense, this means that the Rankine-Hugoniot condition (2.14) are applied to each characteristic on either side.

These conditions, where the shock speed is zero since it is stationary, can simply be expressed as the jump in each characteristic variable. The characteristics has a direction and speed according to the local medium properties, so that values on either enters with upstream and downstream values. This gives the algebraic system for the perturbed quantities (scaled differently than in (3.22)),

$$\bar{\rho}_2\bar{c}_2\big(u^{**} - u^{+}\big) - \big(p^{**} - p^{+}\big) = 0 \tag{3.23a}$$
$$\bar{c}_1^2\big(\rho^{*} - \rho^{-}\big) - \big(p^{*} - p^{-}\big) = 0 \tag{3.23b}$$
$$\bar{\rho}_1\bar{c}_1\big(u^{*} - u^{-}\big) + \big(p^{**} - p^{-}\big) = 0 \tag{3.23c}$$

where the superscript $\pm$ refers to either side of the source, see Figure 3.2.

Everything being linear, the wanted solution at each side of the interface an be

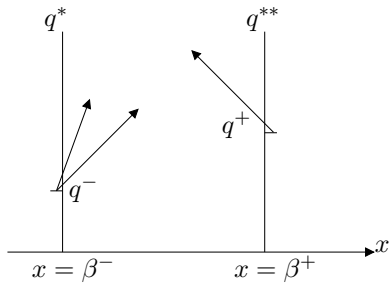

Figure 3.2: The waves entering a source discontinuity

expressed, with $\alpha = \frac{\gamma}{\gamma-1}$, as a linear equation system $Ax = b$, with

$$A = \begin{bmatrix} -\frac{1}{2}\bar{u}_1^3 & \frac{1}{2}\bar{u}_2^3 & -\left(\frac{3}{2}\bar{\rho}_1\bar{u}_1^2 + \alpha\bar{p}_1\right) & \left(\frac{3}{2}\bar{\rho}_2\bar{u}_2^2 + \alpha\bar{p}_2\right) & -\alpha\bar{u}_1 & \alpha\bar{u}_2 \\ -\bar{u}_1^2 & \bar{u}_2^2 & -2\bar{\rho}_1\bar{u}_1 & 2\bar{\rho}_2\bar{u}_2 & -1 & 1 \\ -\bar{u}_1 & \bar{u}_2 & -\bar{\rho}_1 & \bar{\rho}_2 & 0 & 0 \\ \bar{c}_1^2 & 0 & 0 & 0 & -1 & 0 \\ 0 & 0 & \bar{\rho}_1\bar{c}_2 & 0 & 1 & 0 \\ 0 & 0 & 0 & \bar{\rho}_2\bar{c}_2 & 0 & -1 \end{bmatrix} \tag{3.24a}$$

$$b = \begin{bmatrix} q' \\ 0 \\ 0 \\ \bar{c}_1^2\rho^- - p^- \\ \bar{\rho}_1\bar{c}_1u^- + p^- \\ \bar{\rho}_2\bar{c}_2u^+ - p^+ \end{bmatrix} \tag{3.24b}$$

with the solution vector arranged as

$$x = \begin{bmatrix} \rho^* & \rho^{**} & u^* & u^{**} & p^* & p^{**} \end{bmatrix}^T \quad . \tag{3.24c}$$

This system is ill-conditioned with respect to inversion because of the large element scale disparity. In order to avoid this ill-conditioning, the equations are rewritten in terms of nondimensional quantities. The scalings used for this are those presented in the section 2.3 i.e. the inlet values, and this results in the following system

$$A = \begin{bmatrix} -\frac{1}{2}M_1^3 & \frac{1}{2}\left(\frac{\bar{u}_2}{\bar{c}_1}\right)^3 & -\left(\frac{3}{2}M_1^2 + \alpha\frac{\bar{p}_1}{\bar{\rho}_1\bar{c}_1^2}\right) & \left(\frac{3}{2}\frac{\bar{\rho}_2}{\bar{\rho}_1}\left(\frac{\bar{u}_2}{\bar{c}_1}\right)^2 + \alpha\frac{\bar{p}_2}{\bar{\rho}_1\bar{c}_1^2}\right) & -\alpha M_1 & \alpha\frac{\bar{u}_2}{\bar{c}_1} \\ -M_1^2 & \left(\frac{\bar{u}_2}{\bar{c}_1}\right)^2 & -2M_1 & 2\frac{\bar{\rho}_2\bar{u}_2}{\bar{\rho}_1\bar{c}_1} & -1 & 1 \\ -M_1 & \frac{\bar{u}_2}{\bar{c}_1} & -1 & \frac{\bar{\rho}_2}{\bar{\rho}_1} & 0 & 0 \\ 1 & 0 & 0 & 0 & -1 & 0 \\ 0 & 0 & \frac{\bar{c}_2}{\bar{c}_1} & 0 & 1 & 0 \\ 0 & 0 & 0 & \frac{\bar{\rho}_2\bar{c}_2}{\bar{\rho}_1\bar{c}_1} & 0 & -1 \end{bmatrix} \tag{3.25a}$$

$$b = \begin{bmatrix} q'/\bar{\rho}_1\bar{c}_1^3 \\ 0 \\ 0 \\ \tilde{\rho}^- - \tilde{p}^- \\ \tilde{u}^- + \tilde{p}^- \\ \frac{\bar{\rho}_2\bar{c}_2}{\bar{\rho}_1\bar{c}_1}\tilde{u}^+ - \tilde{p}^+ \end{bmatrix} \tag{3.25b}$$

with the tildes denoting nondimensional values. The wanted solution is then found in nondimensional scaling, and at each step, scaled back and fourth. This

scaling reduces the condition number significantly, from $\mathcal{O}(10^6)$ for $M_1 = 0.1$ to $\mathcal{O}(1)$.

The MATLAB built-in direct solver (the backslash operator) is used to solve this linear system, which has to be done at each Runge-Kutta stage. An efficiency improvement would involve the factorization of the coefficient matrix A.
For the inclusion of driver, a linear system is set up in the same way, although the mean flow values do not differ across the source and the right hand side vector has the source term differently. This system is also nondimensionalized.

When the unknowns are solved for, they are used to impose a state solution. This is done the same ways as with boundary conditions, such that the exterior, neighbor solution to the left of the flame is set as $q^+_{\beta^-} = q^*$ and equivalently for the right side, where q denotes either of the three variables.

When a source is zero, the setup system is supposed to give continuous wanted state (no source, no discontinuity). While this is the case for application of the driver system, the heat release calculation does not give continuous wanted states when $q' = 0$. The difference in mean flow states on either side gives, that if the system (3.24) is used for no unsteady heat release, the wanted states are discontinuous. On the other hand, one can argue that if no source is present, why calculate wanted states at all? So in experiments with no unsteady heat release, the numerical flux is applied is its usual fashion.

For the reduced isentropic system (2.15b), only the acoustic waves are present. So the conditions describing their conservation – (3.23a) and (3.23c) – are used, along with the two equations describing the heat input (2.54). These four equations are set up exactly like above.

Validation of basic numerical model

Here the credibility of the scheme is sought validated. The word credibility is used on purpose, since with the used sources and an inhomogeneous medium, a correct spatial convergence test is hard to set up. I should mention that a test on the code for the stagnant medium for spatial convergence has been performed, the setup was a homogeneous medium without any sources, with an acoustic closed end at the left boundary and open at the right. The system was started with a quarter of the fundamental mode and spatial convergence was verified. This test is not included here, primarily the case of a stagnant medium is not really used, except for calculating a reference mode frequency for the frequency drift when a mean flow is included.
The code for the moving medium was sought verified by much the same ap-

proach. In a homogeneous medium without sources, the codes was run with an initial values as the fundamental mode, e.g. for the pressure

$$p'(x, t = 0) = \mathrm{Re}\left\{\left(A\exp(-\imath k_+ x) + A\exp(\imath k_- x)\right)\exp(\imath\omega t)\right\} \tag{3.26}$$

where the Doppler shifted wavenumbers are known $k_\pm = k/1 \pm M$. And the numerical and the analytic solution followed each other during many periods. But the measured maximum error was not as expected, since it was dominated by the error when the analytic solution has its rapid phase change. So I did not included it here.

The overall implementation is still sought validated, in the sense that it gives the correct mode frequency with respect to the analytic frequency when the simulation is post processed. The reference solution used later also has no unsteady heat release as an case. The method has been applied to the same temperature distributions considered with a heat release fluctuation, and these results are presented in the next section.

3.4 Post processing

During the time-simulation, the primitive variables are recorded at each time-step in different positions. These time-series constitutes the data for the frequency analysis. The positions of these series are placed approximately halfways between left boundary and the heat source, halfways between the latter and the driving source, and the last between the driver and the right boundary. All in all 3 times the number of variables. In order to reduce eventual variation between readings at different posistions, the chosen driver is the simpel jump condition for velocity perturbation (2.41), so that minimal entropy fluctuations are generated

At the end of the process, what is wanted is a frequency spectrum, representative for the acoustics in the combustor. In order to do comparison with the analytical solutions, and preferably this being automatized, this spectrum should reveal the main resonance modes present in the overall domain.

So the information from all the time series are sought collected somehow. These series are Hanning windowed before the FFT, not as much to render the signal periodic, but to reduce leakage.
Then a overview of "resonance-behavior" for each spectrum is sought. This is done by searching each spectrum for local maxima, and a sort of hit score is collected, as the number of coinciding maxima.
If a frequency has a local maximum in $\geq 2m + 1$ where m is number of system

variables, then it is treated as found in all spectra and this particular frequency stored. The number of system variables are either 2 or 3. For hits in the interval $2m+1 > x \geq m$, adjacent hits (local maxima) are taken along and a mean value is used as the found resonance frequency. And finally, in the interval $m > x \geq 1$ the same action is performed, except that hits in the surrounding four frequency bins are searched for hits and used to form a mean.

This process will give some uncertainty in the comparison between the numerically and the analytically found resonance frequency, whenever a mean frequency is found. Besides, the numerical found spectras have a certain frequency discretization, dependent on the timestep. So finding the exact frequency down to some decimals is unrealistic. But in general, when the spectra are not to "incoherent", a good estimate of the resonance frequency is found.

Chapter 4

Results

4.1 The Reference Solution

The results from the simulation is analysed in the frequency domain and the resonance frequencies are compared to the "analytic" found resonance frequencies. These latter are found through a derivation, presented in [1], where the sound fields on either side of the flame are set up, isentropic on the upstream side while the downstream sides carries an entropy wave in the density and temperature fluctuations. Along with boundary conditions and the coupling of the fields across the heat source through the RH conditions (2.36), this can be combined into a linear system for the amplitudes of the different waves. For which non-trivial solutions only exists if the determinant is zero.
So this determinant expression (or characteristic polynomial), which has complex entries, is used to find a root in the form of a frequency, so that the system has a solution.

The roots are found by Newton's method, which requires a good starting point in order to converge. This is less optimal in the sense of automation, since it is hard to know in advance what the resonance frequency are. So the start values are given by user by inspection of this complex function when an analytic frequency is sought. The script doing this is not included in the MATLAB codes appendix. The characteristic polynomial was found with MATHEMATICA and is quite large, the derivative even worse.

For the stagnant medium, the possible thermoacoustic oscillations reduced to the roots of $\tan(\omega\beta/\bar{c}_1)\tan(\omega(L-\beta)/\bar{c}_2) = \bar{\rho}_1\bar{c}_1/\bar{\rho}_2\bar{c}_2$ for the case of no unsteady heat, and $\tan(\omega\beta/\bar{c}_1)\tan(\omega(L-\beta)/\bar{c}_2) = \bar{c}_1/\bar{c}_2$ for the type of unsteady heat release, which the author calls 'no unsteady heat input per unit mass' $q' = c_P\big(\bar{T}_2-\bar{T}_1\big)\bar{\rho}_1 u_1'$. The suffices again refers the upstream and downstream values. The same kind of heat sources is used when a mean flow exists i.e. no unsteady heat (at all) and no unsteady heat input per unit mass

$$q' = \Big(c_P\big(\bar{T}_2-\bar{T}_1\big) + \tfrac{1}{2}\big(\bar{u}_2^2-\bar{u}_1^2\big)\Big)\big(\rho_1'\bar{u}_1+\bar{\rho}_1 u_1'\big) \quad . \tag{4.1}$$

4.2 Results

The boundary conditions used in this reference solution is that the outlet is an open end, while the inlet is choked *and* isentropic, i.e. the condition (2.24) and $s' = 0$. The derivation of this solution includes this assumption of isentropic sound field upstream of the flame, so this must be fulfilled in the numerical simulation in order to do comparison.

The hyperbolicity of the system tells us that two boundary conditions are needed at the inflow boundary, so the zero fluctuation mass flux and isentropicity are imposed by setting the velocity and pressure fluctuations as

$$u'(x_{\text{IN}},t) = -\frac{\bar{u}(x_{\text{IN}})}{\bar{\rho}(x_{\text{IN}})}\rho'(x_{\text{IN}},t) \quad \text{and} \quad p'(x_{\text{IN}},t) = \bar{c}^2(x_{\text{IN}})\rho'(x_{\text{IN}},t) \tag{4.2}$$

These imposed states will ensure that no entropy fluctuations are present upstream of the heat release.
In principle, other combinations of used variables could be used to ensure the conditions e.g. ρ' and p'. But then the zero fluctuating mass-flux would give the mean flow in the denominator, and make it less usable for low Mach numbers. This was tried, and it required the time-step to be extremely small in order to have stability at the boundary, and therefore considered useless.

The reduced system (2.15b) only requires one boundary condition at the inlet. Isentropicity is implicitly satisfied, thus the zero fluctuation mass-flux condition is imposed as

$$u'_{\text{Isentropic}}(x_{\text{IN}},t) = -\frac{\bar{u}(x_{\text{IN}})}{\bar{\rho}(x_{\text{IN}})\bar{c}^2(x_{\text{IN}})}p'(x_{\text{IN}},t) = -\frac{\bar{u}(x_{\text{IN}})}{\gamma\bar{p}(x_{\text{IN}})}p'(x_{\text{IN}},t) \tag{4.3}$$

while at the outlet, the same, single condition (pressure release) is used.

So the different tests from section 2.4 are set up with these boundary conditions, and a default geometry. The domain length was take to be a quarter of a

wavelength, the wavelength being determined by the inlet sound speed and the choice of 20 Hz. Inlet temperature is set to around zero degrees Celsius, or $\bar{T}_1 = 273$ K. The inlet pressure is set to 10^5 Pa, by which the density is found. The mean velocity scales with the inlet Mach number, which is one of the tunable parameters. When simulating with a mean flow, this is taken in the interval $1.5 \cdot 10^{-4} \leq M_1 \leq 0.15$. And the other parameter, the downstream temperature is taken in the interval $\bar{T}_1 + 50 \text{ K} \leq \bar{T}_2 \leq \bar{T}_1 + 550 \text{ K}$.

The discretization used in the experiments is 16 elements of 4'th order approximation, which is more than enough to resolve the waves in the system. When all the simulations were run, this was chosen to absolutely guarantee a sufficient resolution. When used as a simulation to get an estimate of the thermoacoustic modes, a lower discretization is sufficient, of course considering the frequency range.

The chamber is driven by the sweep signal in the range 10-110 Hz, and after a signal-period ($1s$), the recorded time-series are Fourier transformed to get the power spectra. The resonance frequencies are then identified and compared. The reference solution does, to the best of my knowledge, not assume a constant mean pressure. The equations are solely described by mean velocities and densities, sound speeds and temperatures. Of course, the mean pressure has an implicitness, but if the mean flow values are consistent, this should not do any difference.

While for the reduced system, hopefully there is no difference. The unsteady heat release effect is included through the reduced RH conditions (2.54), which should describe the influence just as well for this reduced system. As long as the entropy wave does not interact with boundary conditions and such, the two cases should be equal.

The data are presented as the shift in frequency with respect to that particular frequency in the stagnant medium. This is to show the mean flow effects, and scale down the results. In a figure, the x-axis is the inlet Mach number, while the y-axis is divided into bands. Each band represent a temperature difference across the heat input, where the middle of these bands is the reference no flow frequency (a dotted line), and the full lines surrounding this is a deviation of ± 5 Hz. The lines with square markers is the deviation of exact frequency, while the 'x' markers denotes the numerically found resonances. If no frequency is found from the simulations near that particular frequency, this case of $\left(M, \Delta\bar{T}\right)$ is left out.

The presented figures are unfortunately not very precise in terms of exact deviation, but it is possible to distinguish between deviations of 2 and 4 Hz. Besides, the exact numbers are less useful, it is tendencies that are interesting.

Starting with the comparison between the two cases of mean pressure distribution in Figure 4.1 which is without the unsteady heat source . It can be faintly seen that there is a small deviation in drift frequency, also in the analytic frequency, but it is for larger Machs and temperature jumps only. It is not much, but if the frequency range was broadened, it would probably be more visible.
In addition to that, the numerical method simulates the oscillations rather well, there is no sign as such of bad wave propagation. It should be mentioned that the third resonance frequency ~ 160 Hz, lies outside the frequency range of the excitation signal, but is nevertheless well excited.

Then is looked at the reduced system. In Figure 4.3 and Figure 4.4 is compared the reduced system with the full, without and with unsteady heat release respectively and both with a constant mean pressure distribution. From these it is clear that the reduced system in this particular setup does equally well. There is a small deviation from the exact frequency in the first resonance mode when the heat source is present, but this applies to both the reduced and the full system. So it could be justified to settle with the computationally less expensive reduced system.

Finally, inspecting Figure 4.2, Figure 4.5 and Figure 4.6 reveals a surprise. That the drop in mean pressure has an negative effect when the heat source is present, whether it be the full or the reduced system. The reduced system is affected in higher frequencies even without having the heat source included. Figure 4.2 which shows the full system with heat source and constant versus changing pressure reveals quite large deviation, in all the resonances considered and even for the smallest temperature change. And even more strange is that this effect does not get smaller for $M \to 0$, where the mean flow distributions coincides.

I don't think it is question of a flaw in the numerical model, there is no signs of odd computations as such, all matrices to be inverted are very well conditioned and no spurious oscillations or something like that has been noticed. And that it shows an influence on the reduced system without heat release, where no computations as such are performed over the material interface, is even more mystifying.
It could be the data collecting, if the spectra had resonances distributed over a small interval, and hence find mean values not really representative. But the searching of the spectra has been "monitored", i.e. the found frequencies was indicated in the spectra and inspected, and no deviation was found that could explain this. Or else it is the expression that is used to calculate the pressure change which is unphysical, but this also seems unreasonable. An issue for further study, must be the conclusion for now.

Finally a short example of the mentioned acoustic instability is presented. This

is generate simply by changing the inlet boundary conditions, so that these are fixed mass flux along with pressure release. The outlet is still open. These inlet conditions does not ensure isentropicity in the upstream field, and an entropy wave is present. This affects the unsteady heat release, since this is dependent on the density fluctuation. The resulting spectrum only contains this unstable mode which can be seen in Figure 4.2 along the spectrum resulting from requiring isentropic boundary conditions. The inlet Mach number is set to 0.05 and $\Delta\bar{T} = 200$. The spectra are normalized, so it is not evident that it really is an instability, but after $0.3s$ the pressure levels were $> 10^4$. The stable spectrum also shows the different signals, while the unstable only has this all-dominating peak.

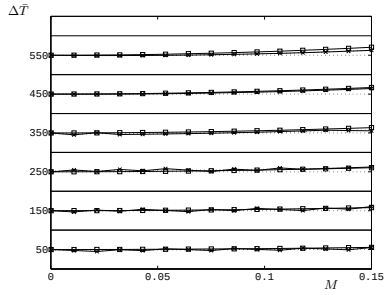

(a) 1. resonance frequency

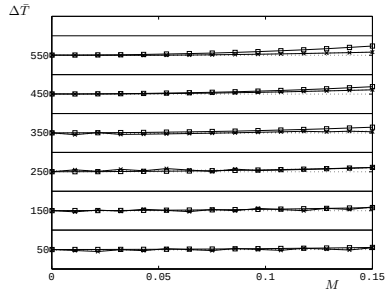

(b) 1. resonance frequency

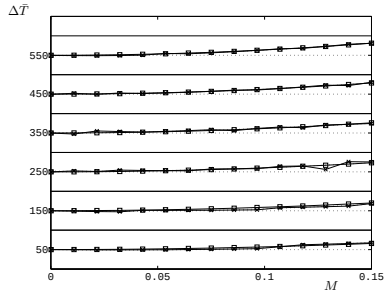

(c) 2. resonance frequency

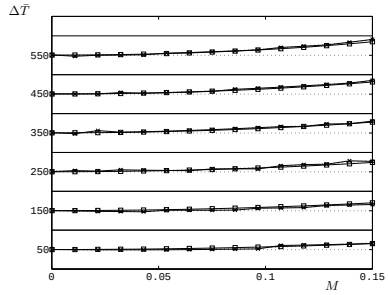

(d) 2. resonance frequency

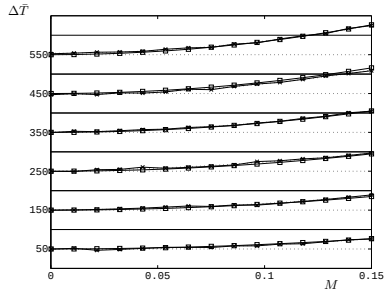

(e) 3. resonance frequency

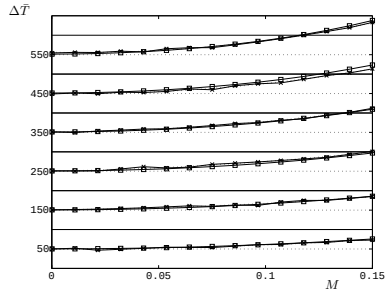

(f) 3. resonance frequency

Figure 4.1: Full system, no unsteady heat, constant pressure in left column, pressure drop in right

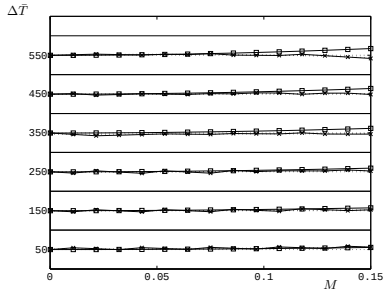

(a) 1. resonance frequency

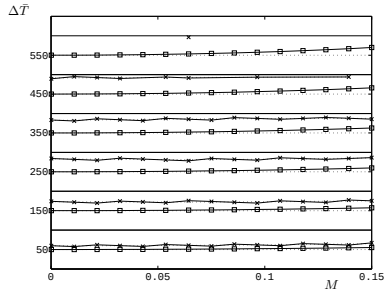

(b) 1. resonance frequency

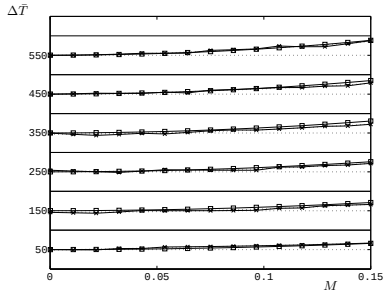

(c) 2. resonance frequency

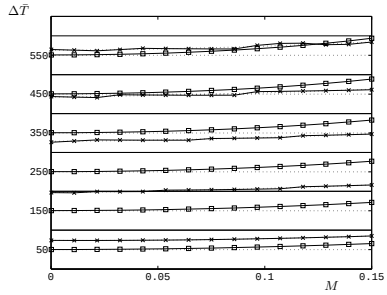

(d) 2. resonance frequency

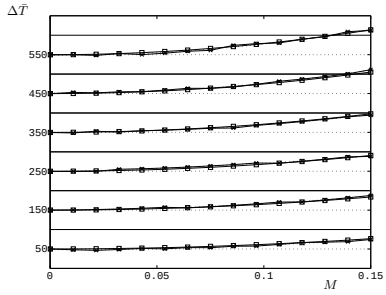

(e) 3. resonance frequency

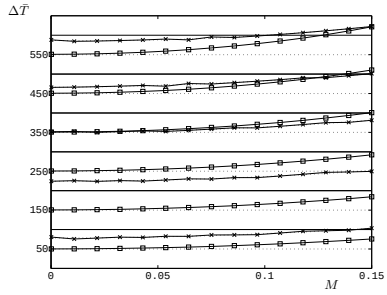

(f) 3. resonance frequency

Figure 4.2: Full system, Unsteady heat, constant pressure in left column, pressure drop in right

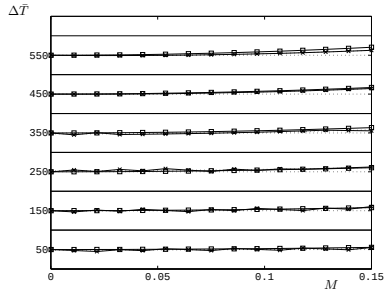

(a) 1. resonance frequency

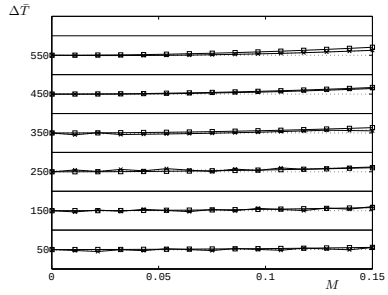

(b) 1. resonance frequency

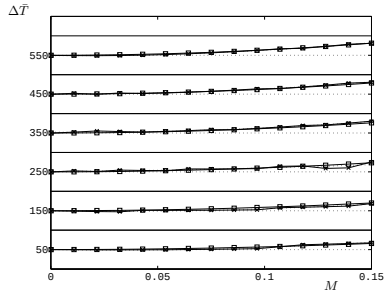

(c) 2. resonance frequency

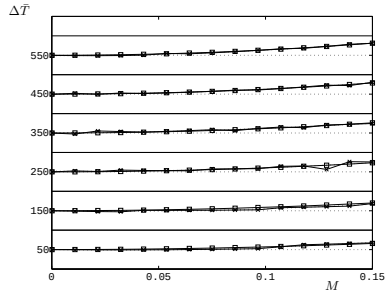

(d) 2. resonance frequency

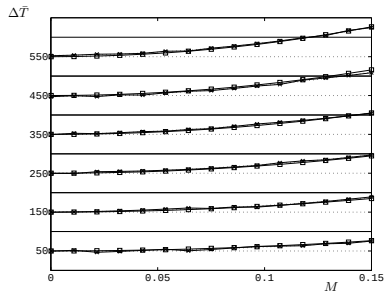

(e) 3. resonance frequency

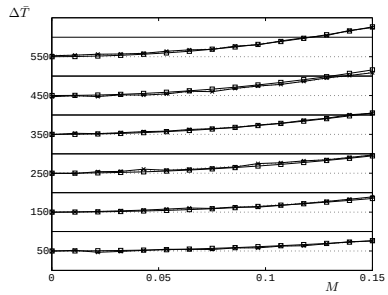

(f) 3. resonance frequency

Figure 4.3: Reduced system in left, Full in right, No unsteady heat, constant pressure

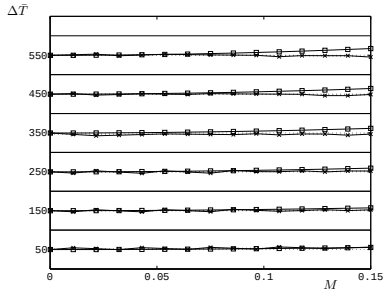

(a) 1. resonance frequency

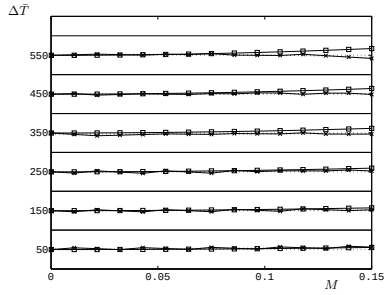

(b) 1. resonance frequency

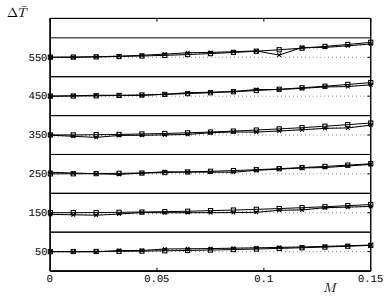

(c) 2. resonance frequency

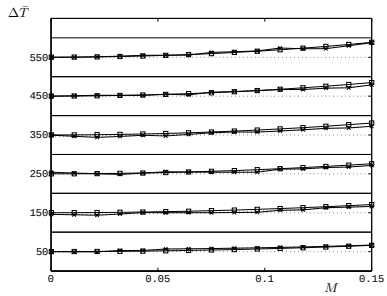

(d) 2. resonance frequency

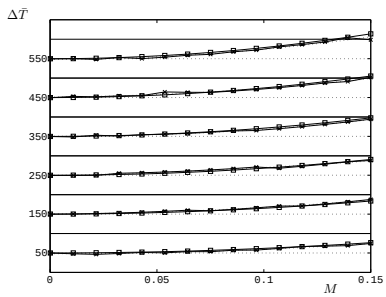

(e) 3. resonance frequency

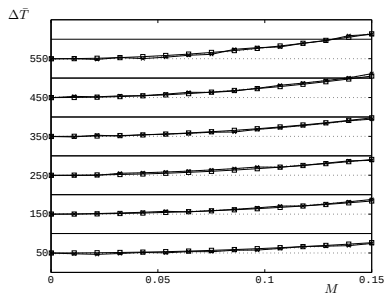

(f) 3. resonance frequency

Figure 4.4: Reduced system in left, Full in right, Unsteady heat, constant pressure

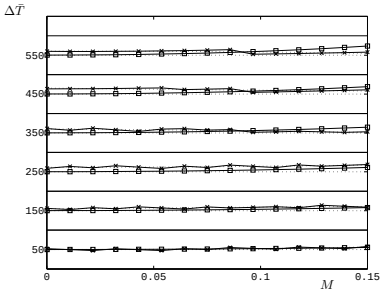

(a) 1. resonance frequency

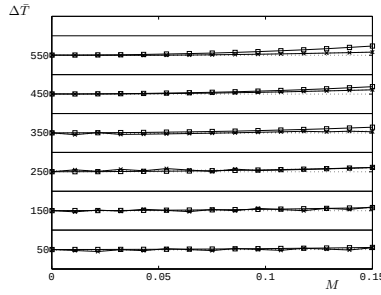

(b) 1. resonance frequency

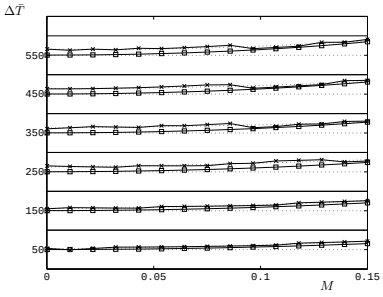

(c) 2. resonance frequency

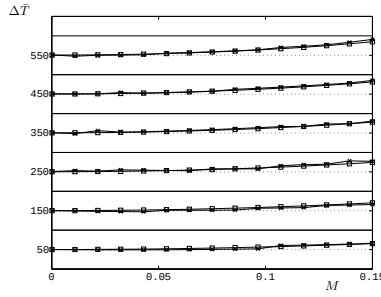

(d) 2. resonance frequency

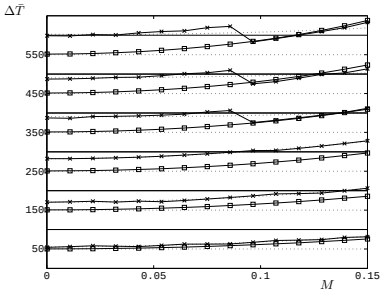

(e) 3. resonance frequency

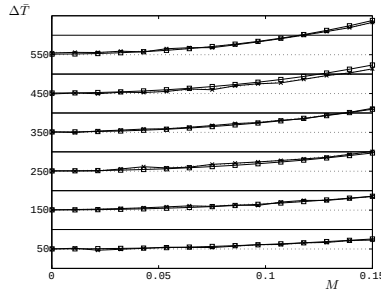

(f) 3. resonance frequency

Figure 4.5: Reduced system in left, Full in right, No unsteady heat, pressure drop

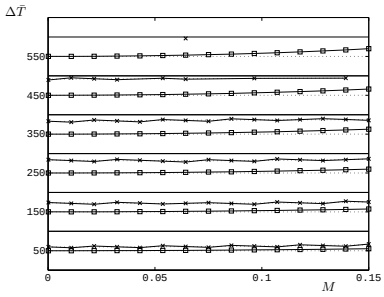

(a) 1. resonance frequency

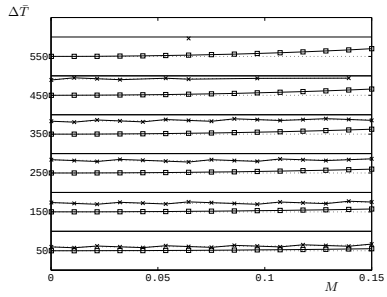

(b) 1. resonance frequency

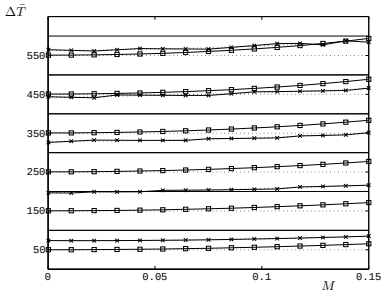

(c) 2. resonance frequency

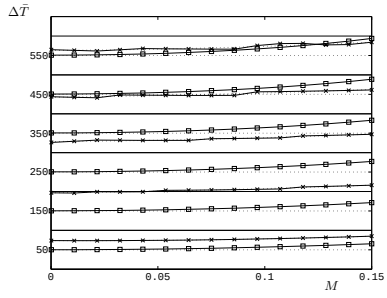

(d) 2. resonance frequency

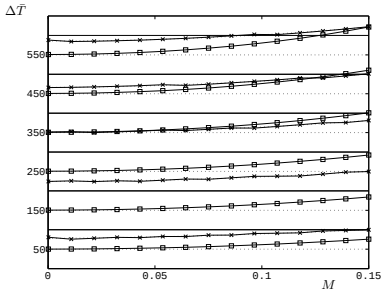

(e) 3. resonance frequency

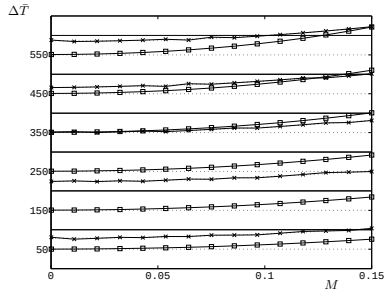

(f) 3. resonance frequency

Figure 4.6: Reduced system in left, Full in right, Unsteady heat, pressure drop

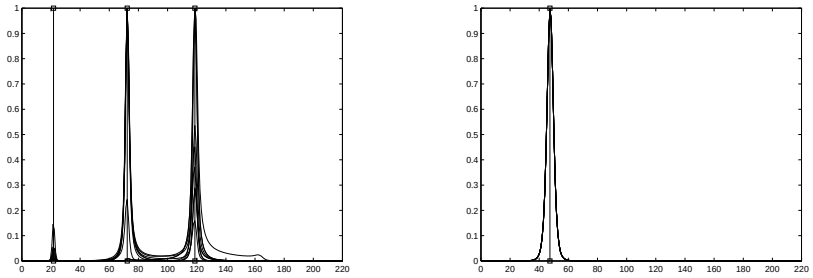

(a) Stable (b) Unstable

Figure 4.7: Normalized spectra of thermoacoustic oscillations

4.3 Conclusion

In this report was presented the general acoustical theory regarding environments where the sound field is affected by exchange of heat. The level of abstraction in terms of the actual combustion was quite high, treating it as an energy source only. The resulting model for the acoustics was the linearized Euler equations with a source term, representing a fluctuating heat release which acts as a sound source. The placement of such a source within a acoustically closed system constitutes the used governing model for thermoacoustic oscillations in an idealized model of a combustor.

The physically based conditions known as the Rankine-Hugoniot conditions, describing the balance of energy flux across a heat release was used to in linearized form to incorporate an unsteady heat release source into the numerical method, used to simulation of the acoustics.

The numerical method used to discretize the governing equations in space was the discontinuous Galerkin method. The method is based on domain decomposition into elements, and a polynomial approximation on these. It has the advantage of not requiring continuity across these elements. This property was used to include the unsteady heat release as a compact source inbetween elements. The general approach to include acoustical compact sources in the method, is to combine jump conditions describing physics with conditions on the characteristic waves in the system.

The model of the scenario being very simple with uniform properties on either

side of the heat source, was used to validate that the numerical model is capable of representing such a resonator model and the possible modes. A sound field was generate through included driver sources, and the acoustic fluctuations was recorded in order to do frequency analysis. Comparison with analyticly found resonance frequencies showed that within the overall method, including data collecting, the method was able to capture the thermoacoustic modes within a few hertz.
The advantage of using numerical simulations in the time-domain relies on the possible excitation of many modes simultaneously.

The implementation of the analysis method in this project is a start, but far from sufficient to be used a diagnostic tool. Although some different boundary conditions used frequently in the modelling of such system is included, it does not deal with more realistic scenarios. Also the searching algorithm for resonances in the time-series could be improved or done otherwise. But the numerical scheme itself with the source inclusion, has shown to an effective method, and since it is quite flexible, it can surely be applied to more complicated thermoacoustic problems.

Bibliography

[1] A.P. Dowling. The calculations of thermoacoustic oscillations. *Journal of Sound and Vibration*, 180(4):557–581, 1995.

[2] Jan S. Hesthaven and Tim Warburton. *Nodal Discontinous Galerkin Methods: Algorithms, Analysis and Applications*. Springer, To Appear.

[3] S.W. Rienstra and A. Hirschberg. *An Introduction to Acoustics*. `http://www.win.tue.nl/~sjoerdr/papers/boek.pdf`, 15th April 2005.

[4] O.M. Umurhan. Exploration of fundamental matters of acoustic instabilities in combustion chambers. *Center for Turbulence Research, Stanford, Annual Research Briefs*, 1999. `http://ctr.stanford.edu/ARB99.html`.